2017

Determining the effects of methanol, ethanol, isopropanol, and glycerol on both thermal stability and catalytic activity of Rv0045c, an enzyme from M. tuberculosis

Katelyn Baumer
Butler University

BUTLER UNIVERSITY HONORS PROGRAM

Honors Thesis Certification

Please type all information in this section:

Applicant Katelyn Baumer

Thesis title Determining the effects of methanol, ethanol, isopropanol, and glycerol on the thermal stability and catalytic activity of Rv0045c, an enzyme from *M. tuberculosis.*

Intended date of commencement May 6, 2017

Read, approved, and signed by:

Thesis adviser(s) Geoffrey C Hoops Geoffrey C. Hoops 4/28/2017
Date

Date

Reader(s) 5/1/2017
Date

Date

Date

Certified by
Director, Honors Program Date

For Honors Program use:

Level of Honors conferred: University

Departmental

Determining the effects of methanol, ethanol, isopropanol, and glycerol on both thermal stability and catalytic activity of Rv0045c, an enzyme from *M. tuberculosis*

A Thesis

Presented to the Department of Chemistry

College of Liberal Arts and Sciences

and

The Honors Program

of

Butler University

In Partial Fulfillment

of the Requirements for Graduation Honors

Katelyn Marie Baumer

May 6, 2017

Table of Contents

Abstract

Tuberculosis (TB) is a highly infectious respiratory disease contracted through the inhalation of *Mycobacterium tuberculosis*. Serine hydrolases are abundant in *M. tuberculosis* and serve as a model for studying the inhibition of TB. Rv0045c is an example of such with little known regarding its biological function. Rv0045c was exposed to methanol, ethanol, isopropanol, or glycerol and the effects of varying concentration of these alcohols on the catalytic efficiency and thermal stability of the enzyme was determined. The thermal stability of Rv0045c was found to decrease with concentration of methanol, ethanol, or isopropanol. The opposite was true of the thermal stability when exposed to increasing concentrations of glycerol. The effect of the alcohols on enzyme kinetics, however, were much less straightforward. Data suggests that a concentration of 10% alcohol by volume is optimal for catalytic activity.

Introduction

Tuberculosis (TB) is a highly infectious respiratory disease which affects millions of people worldwide. In 2014 alone, there were nearly 10 million cases of the disease and 1.5 million of those cases lead to death. [1] The disease is caused by inhalation of *Mycobacterium tuberculosis*, bacteria that are able to survive only in humans and typically infect the lungs as it is an aerobic bacteria and thus needs oxygen to survive. [2] It is possible for an individual to become infected by *M. tuberculosis* and not show symptoms of infection for years; this is because the bacteria are able to remain dormant inside human tissue, giving rise to what is known as a latent TB infection. [2] This is one of many factors that adds to the challenge of fully understanding and treating TB. The antibiotic-resistant nature of *M. tuberculosis* is also particularly concerning in developing treatment for the infection. In 1998, the complete genome of *M. tuberculosis* was sequenced at the Sanger institute so that a better understanding of TB could be obtained and new knowledge could be applied to the improvement of treatment options for the infectious disease. [3] One of the approximately 4,000 genes found codes for the protein Rv0045c, which serves as the main focus of this study.

Many years after Rv0045c was found to be present in the *M. tuberculosis* genome, the protein was further characterized in 2010. [4] In this study, Rv0045c was shown to be a catalyst for the hydrolysis of esters. Further experimentation regarding activity and stability of Rv0045c supported this as well, leading to the conclusion that Rv0045c is an esterase. [4] It was later determined that the enzyme is more specifically a serine hydrolase, an enzyme which utilizes a nucleophilic serine residue to break ester and amide linkages. [5] Additionally, the main catalytic residues of other known esterases

of this family are highly conserved in Rv0045c. [4] In 2011 the crystal structure of Rv0045c was determined through via X-ray diffraction. [6] They determined that the structure is highly characteristic of the previously mentioned α/β-hydrolase family, an 8-stranded β-sheet which is parallel, except for the second strand which is antiparallel, surrounded by α-helices. Additionally, a cap domain was discovered to have two α-helices and two β-strands. [6] Researchers also used sequence alignment and structural homology to determine the active site of Rv0045c, finding that the active sight includes a serine at residue 154 and histidine at residue 309. [6] Despite determining the structure of the majority of the protein, researchers were unable to visualize the flexible loop of residues 194-204, which covers the binding site (Figure 1, magenta). [6]

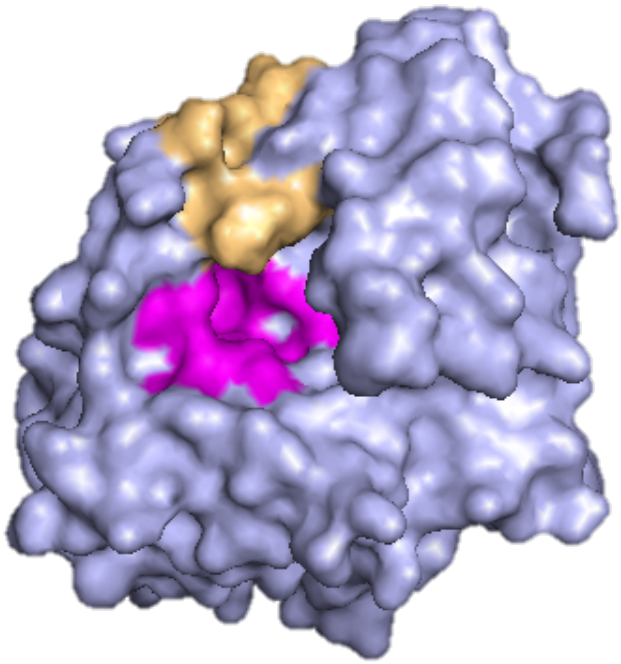

Figure 1: Rv0045c structure including flexible loop. Light orange = flexible loop; magenta = binding pocket.

The flexible loop was later modeled through mutational analysis and kinetic assays (Figure 1, light orange). [7] In this study, alanine screening mutagenesis was used

to identify flexible loop residues important to catalytic activity. Relatively low variation in thermal stability of the protein in response to mutations of residues within the loop indicated that it was a flexible, random loop. However, the introduction of some mutations significantly altered the catalytic activity, indicating that the loop played an important role in the active site, whether it be through binding or orienting of the substrate. [7] It was determined that Val 198 and Leu 200 were critical to activity levels and were oriented towards the center of the active site, while other amino acids with seemingly no role in catalysis pointed away from the active site. This suggests that Rv0045c has an enclosed hydrophobic binding pocket similar to that of ybfF [8], a similar hydrolase from *V. cholerae*. It was also determined that Gly90 and His187 play a substantial role in the substrate selectivity of the enzyme. [7]

After the protein had been adequately characterized, unpublished data from a spring 2013 CH463 biochemistry laboratory class at Butler University 2013 suggested that the presence of alcohol may affect the activity of Rv0045c, though further research was necessary to confirm these results. Additionally, previous research has shown that enzyme activity levels are often slightly altered in the presence of alcohols. Glycerol kinase activity has been previously shown to decrease in the presence of ethanol accumulation. [9] Previous studies have shown that glycerol is capable of affecting enzyme activity, though there is little consistency in whether activity is regulated up or down. For example, Carboxylesterases have previously been shown to exhibit modest increases in activity levels in the presence of glycerol. [10] However, creatine kinase isolated from rabbit muscle has previously been shown to exhibit slight decreases in activity. [11] This study will aim to investigate the effects of alcohols on both activity and

thermal stability of Rv0045c. The effects of methanol, ethanol, isopropanol, and glycerol on the thermal stability of Rv0045c will be measured using differential scanning fluorimetry (DSF) and the effects of the same alcohols on the catalytic activity of Rv0045c will be determined using a fluorescein based kinetic assay.

Materials and Methods

Overexpression and Purification of Rv0045c Protein

The Rv0045c protein analyzed throughout this project is overexpressed in *E. coli* and purified. The protein, which has an N-terminal 6x His-tag, was overexpressed using a derivative [4] of the commercial plasmid pET28a which carries the Rv0045c gene from *M. tuberculosis*. The plasmid was transformed into *E. coli* BL21(DE3) RIPL cells and cultured to saturation overnight at 37°C in LB media treated with kanamycin and chloramphenicol to prevent contamination. These cells were then transferred to 250mL of LB media and grown at 37°C with constant shaking at 225rpm until mid log phase were reached (Absorbance= 0.6-0.8). Temperature of the culture was then decreased to 16°C and IPTG was added to a final concentration of 1.0mM. Cells were centrifuged at 5000g for 10 minutes at 4°C and resuspended in PBS.

Approximately 50mg of lysozyme and 1.5 mL of 10x Bug Buster were added to the suspension which was then rotated at 4°C for 2-3 hours to allow the cells to lyse completely. Cells were then centrifuged at 18000g at 4°C for 10 minutes to remove unwanted cellular material. 600µL Ni-NTA agarose resin was added to the supernatant and the solution rotated for 20 minutes at 4°C. The resin was then washed with increasing concentrations of imidazole (40mL of 10mM, 25mM, or 50 mM imidazole in PBS) and centrifuged at 2500g for 1 minute. Supernatant was removed entirely and resin was washed once more with 3.0mL of 250mM imidazole to release the protein from the resin. The protein was allowed to dialyze overnight in phosphate buffered saline pH 7.4 (PBS).

Absorbance at 280nm of the dialyzed protein solution was measured and converted to molarity with an extinction coefficient of ε^{280}= 35980 $M^{-1}cm^{-1}$ to determine

the concentration of the protein collected. The purity of this protein is then determined through SDS-PAGE. Protein was considered viable if purity was great than or equal to 95%.

Measuring Thermal Stability

The effect of various alcohols in increasing concentrations on Rv0045c stability was determined through differential scanning fluorimetry, as described previously. [12,13] Rv0045c (4μL of 3.0μg/mL), a 1:200 dilution of SYPRO Orange fluorescent dye (2μL), alcohol of the desired concentration (2μL), and Phosphate buffered saline pH 7.4 (PBS) buffer (19μL) were loaded into a 96 well plate in triplicate. Temperature was increased from 15°C to 80°C in 1°C increments in a BioRad Thermocycler. Thermal stability was then determined by graphing the negative derivative of the fluorescence, of which the local minimum corresponds to the melting point of the enzyme (Appendix A).

Measuring Catalytic Activity

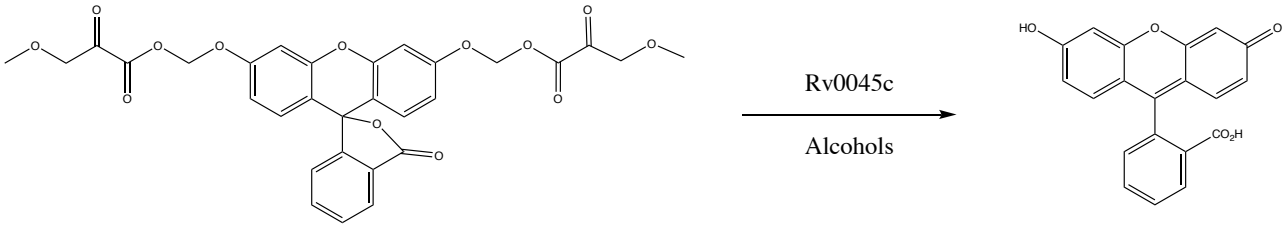

Methoxyacetic Fluorescein Derivative (MOAME)
(non-fluorescing)

Fluorescein

Figure 2: Rv0045c catalyzed hydrolysis of the fluorogenic substrate MOAME resulting in fluorescein

Rv0045c catalyzed hydrolysis of MOAME, an ester linkage-modified non-fluorescent fluorescein derivative, produces the fluorescent compound fluorescein [14,15]

(Figure 1), giving rise to kinetic data useful in determining the catalytic activity of the enzyme. This fluorescence assay was completed in a 96-well microplate using a Synergy H1 Hybrid Reader and data was collected with the Gen 5 software. Acetylated bovine serum albumin (BSA) (0.1mg/mL) was included in all wells to prevent the non-specific binding of Rv0045c to the well plate. Solutions of varying methanol ethanol, isopropanol, or glycerol concentrations were created by adding the appropriate volume of alcohol to PBS+BSA buffer. In order to include a fluorescein standard curve one column per every triplicate assay at a fixed concentration of alcohol contained eight two-fold serial dilutions of fluorescein in PBS+BSA with alcohol. Each remaining column was used to create two-fold serial dilutions of MOAME with an initial concentration of 100μM in PBS+BSA with alcohol. This is done in triplicate for each alcohol concentration. Rv0045c protein was diluted to a concentration of 100μg/mL, 5μL of which is added to each substrate-containing well, yielding a final concentration of 141nM. Once enzyme had been added to the appropriate wells, the 96-well plate was quickly loaded into the fluorescent plate reader with an internal temperature of 28°C and kinetic analysis was started immediately. The data was then processed to plot steady state reaction rate versus substrate concentration and is fit to a Michaelis-Menten curve in Origin 6.1 software. The curve reveals values for the K_M and V_{max} of which V_{max} is then used to calculate k_{cat} by dividing by the enzyme concentration. The k_{cat}/K_m ratio is calculated as a measure of catalytic efficiency.

Results and Discussion

DSF was used to determine the thermal stability of Rv0045c in the presence of methanol, ethanol, isopropanol, or glycerol, in concentrations ranging from 0-60% by volume for glycerol and 0-30% by volume for all other alcohols.

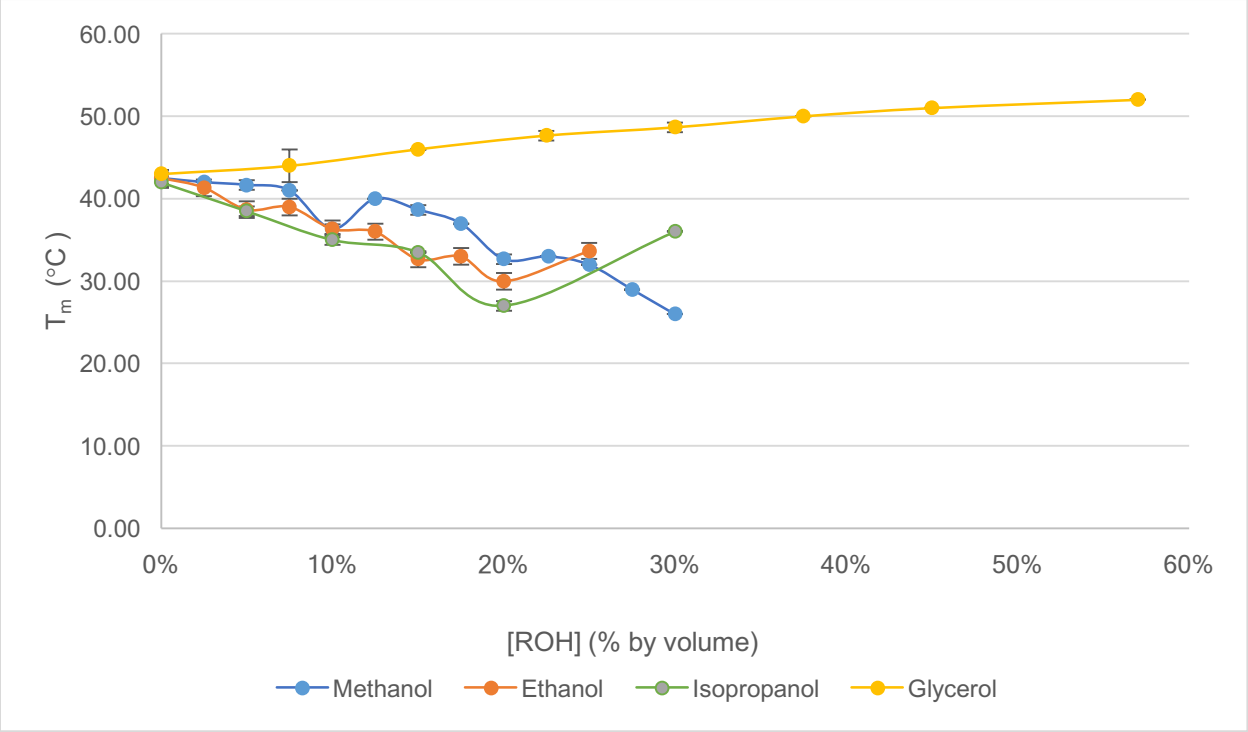

Figure 3: Effect of methanol, ethanol, isopropanol, and glycerol on thermal stability of Rv0045c.

Differential scanning fluorimetry was used to determine the thermal stability of Rv0045c in the presence of various alcohols at increasing concentrations. Wild type Rv0045c in the presence of no alcohol has a T_m of between 42-43°C; in the presence of methanol, ethanol, or isopropanol this decreased to values ranging from 27-32°C. The opposite effect was observed in the presence of glycerol. T_m increased to a value of 52°C in the presence of 57% glycerol. Values were not obtained for the T_m of Rv0045c in the presence of methanol, ethanol, or isopropanol at concentrations greater than 30% by volume due to limitations of the assay.

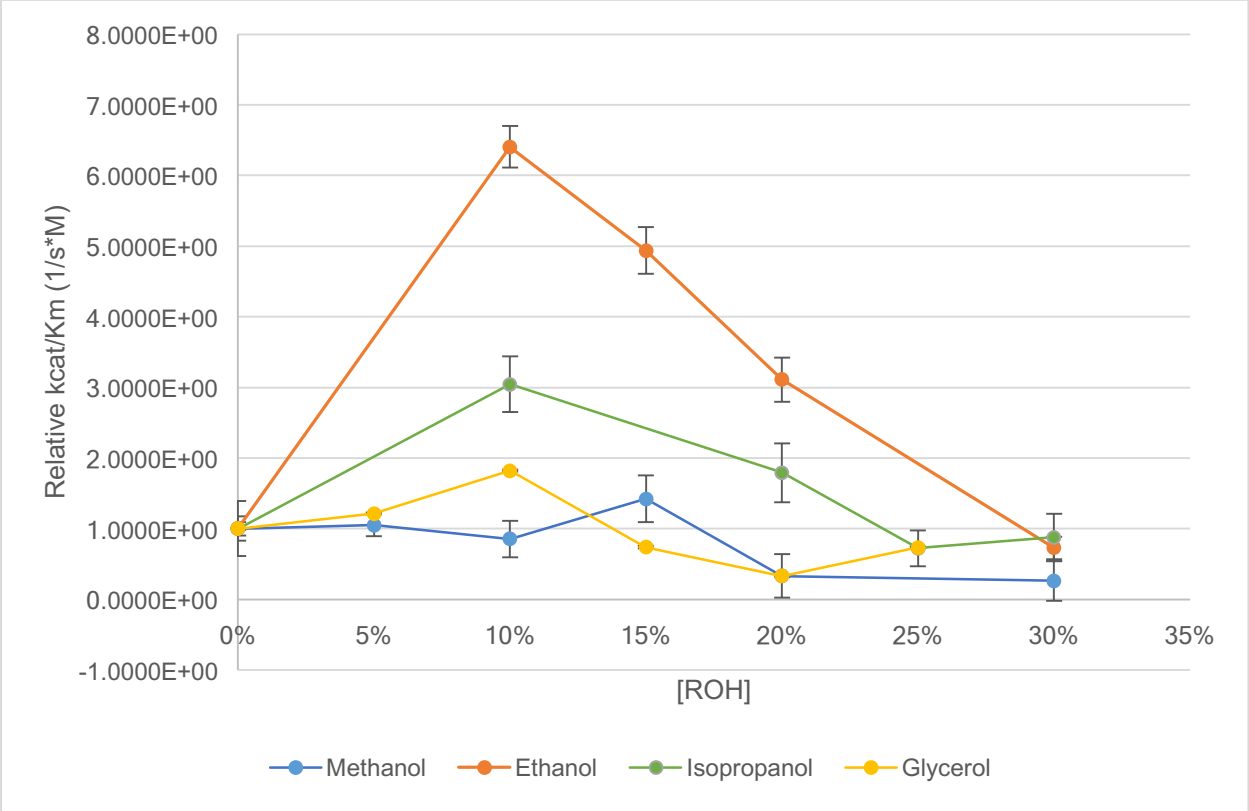

Figure 4: Effect of methanol, ethanol, isopropanol, or glycerol on the enzymatic activity of Rv0045c.
Enzymatic activity in the presence of alcohol was determined by fluorogenic kinetic assay. Rv0045c experienced optimal activity in the presence of 10% alcohol by volume for each alcohol tested with the exception of methanol. Activity then decreased to a level below that of Rv0045c in the presence of no alcohol. Values shown are relative to the k_{cat}/K_m value determined in the presence of no alcohol to normalize differences between assays.

Glycerol

Results for glycerol were generally opposite of those of the other alcohols. As expected, the presence of glycerol increased the thermal stability of Rv0045c from 43°C when no alcohol was present to 52°C when there was 57% glycerol by volume (Figure 4). This increase in thermal stability may indicate that glycerol can be used to store purified Rv0045c protein at temperatures below 0°C in the laboratory.

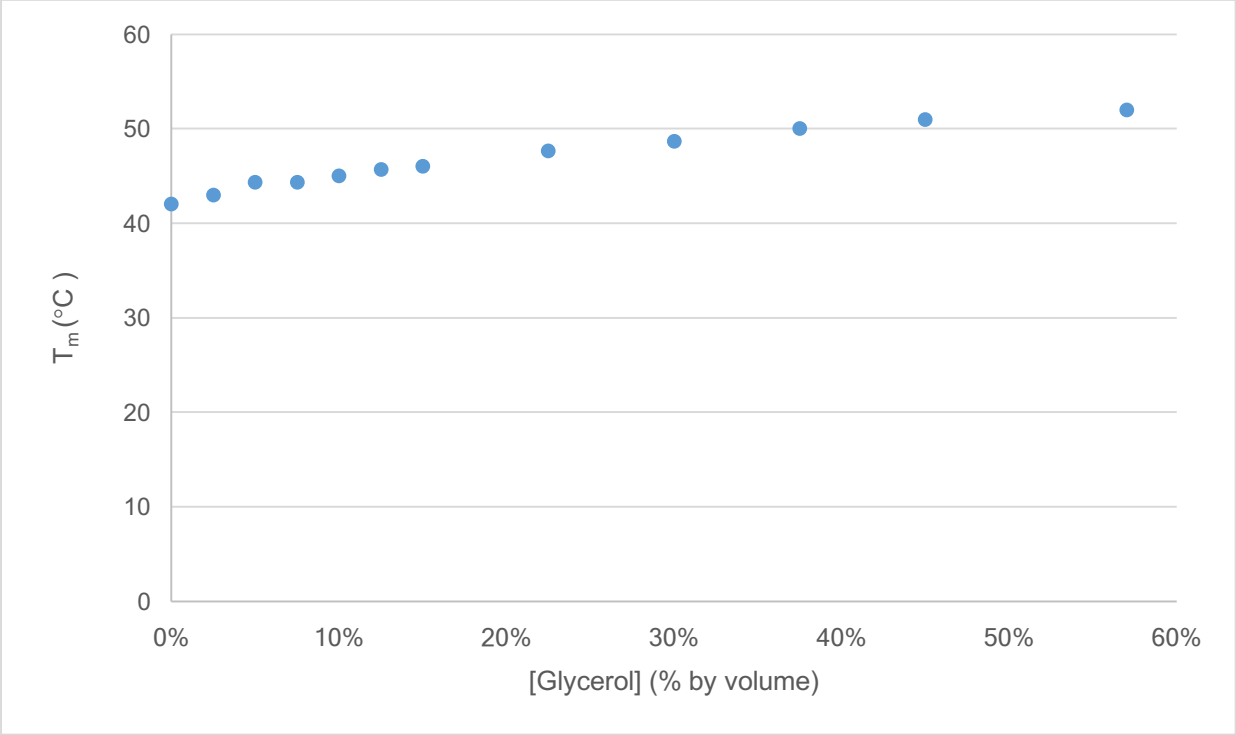

Figure 5: Presence of glycerol increases the thermal stability of Rv0045c.

Differential Scanning Fluorimetry (DSF) with SYPRO Orange was used to determine the "melting point" of Rv0045c. Melting Points shown are the average of three replicates. Increasing concentrations of glycerol yielded a steady increase in thermal stability of the enzyme.

Despite the increase in thermal stability, there was no consistent trend in the effect of glycerol concentration on the activity levels of Rv0045c as determined through fluorogenic kinetic assays (Figure 5). k_{cat}/K_m ranged from 92.8 $s^{-1}M^{-1}$ the presence of 20% glycerol to 511.1 $s^{-1}M^{-1}$ in the presence of 10% glycerol. It was expected that a stability increase in response to glycerol may correspond to a similar increase in catalytic activity, however the effect of glycerol on catalytic activity did not show a steady increase or decrease in activity. Rather, catalytic activity increased substantially between 0% and 10% glycerol by volume, then decreased as glycerol concentration surpassed 10% by volume and falling below the k_{cat}/K_m ratio observed in the presence of no alcohol. This was unusual, but similar kinetic results when the assay was completed with other

alcohols suggests that there may be an optimal alcohol concentration for Rv0045c activity. In concert, these results lend themselves to the possibility of storing Rv0045c in glycerol rather than simply in PBS buffer to extend the window of time in which Rv0045c can be used following purification. Since the range of catalytic activity in the presence of differing concentrations of glycerol extends above and below that of the enzyme in the absence of alcohol it would be possible to determine an optimal glycerol concentration at which Rv0045c can be stored to both extend the life of the purified protein and have minimal if any effect on the activity of the enzyme for use in other assays. It has the potential to be very useful in a laboratory setting to save a large amount of time and resources.

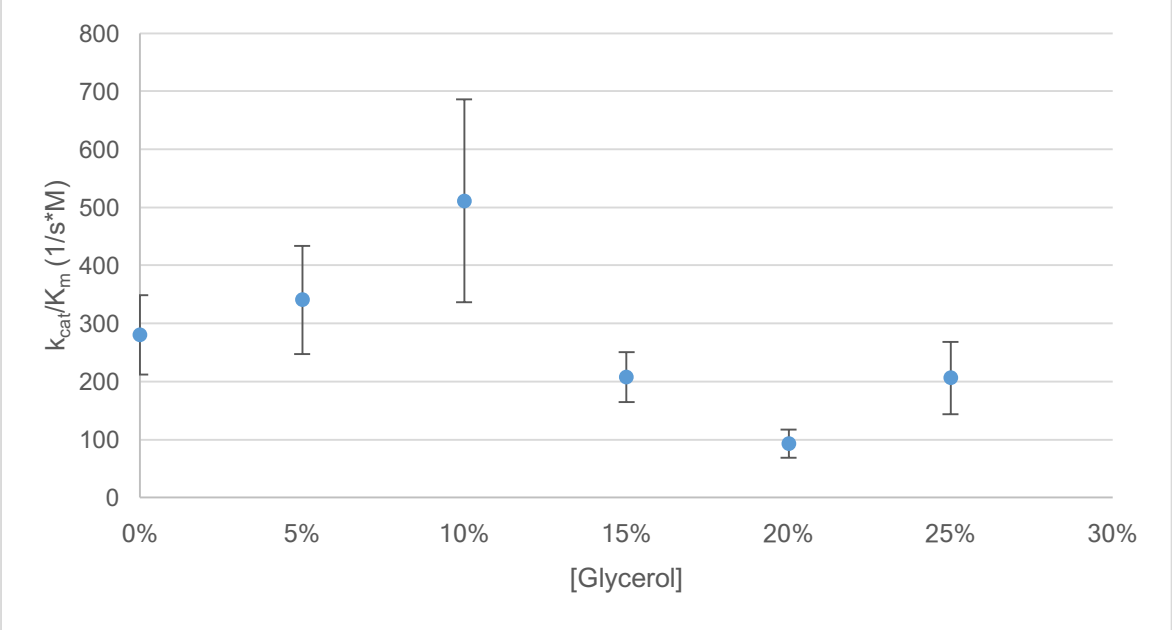

Figure 6: Effect to glycerol on catalytic efficiency of Rv0045c.

A fluorogenic kinetic assay was used to analyze the catalytic efficiency of Rv0045c. The average of three replicate reaction rates of the hydrolysis of MOAME was plotted against [MOAME] in Origin 6.1 software to produce a hyperbola to fit standard Michaelis-Menten kinetics. K_m and k_{cat} were calculated and used to determine the catalytic efficiency of the enzyme. Increasing glycerol concentrations had no consistent effect on the overall catalytic efficiency.

Methanol

Increasing methanol concentration steadily decreased the thermal stability of Rv0045c. DSF showed a change in T_m from 42.5°C when in the presence of no alcohol to 26°C in the presence of 30% methanol (Figure 6). T_m values for Rv0045c in the presence of methanol concentrations equal to 10%, 20%, and 30% do not align exactly with the rest of the data. It is important to note that these three measurements were collected in the same assay which was separate from the assays containing all other data points. It is likely that a single source of error is responsible and this data does not suggest a rise and fall of T_m as it may appear in Figure 4. Results are only reliable at concentrations of methanol less than or equal to 30% by volume. Once this concentration was exceeded, the environment became so hydrophobic that SYPRO Orange was able to fluoresce prior to the denaturation of Rv0045c, eliminating the possibility of measuring a change in fluorescence and determining the true T_m of Rv0045c at higher alcohol concentrations.

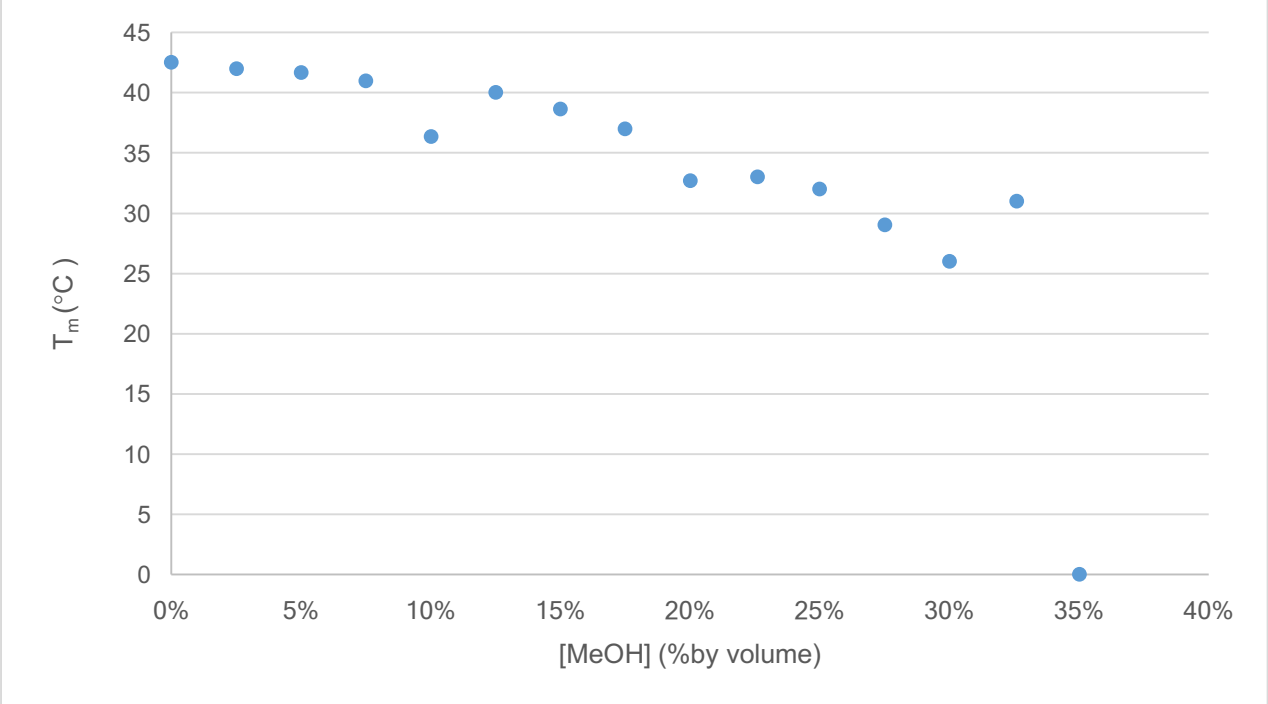

Figure 7: Presence of methanol decreases the thermal stability of Rv0045c.

Differential scanning fluorimetry (DSF) with SYPRO orange was used to determine the "melting point" of Rv0045c. Melting points shown are the average of three replicates. Increasing concentrations of methanol yielded a steady decrease in thermal stability of the enzyme. Melting point could not be determined at [MeOH] > 30% due to limitations of the instrument to detect a change in fluorescence in a highly hydrophobic system.

Similarly to thermal stability, the catalytic activity of Rv0045c appeared to decrease in the presence of increasing concentration of methanol (Figure 7). However, as was observed with glycerol, the highest k_{cat}/K_m in the presence of methanol was observed when 15% alcohol was present. This value was equal to 1352 $s^{-1}M^{-1}$. The lowest observed k_{cat}/K_m was equal to 249.7$s^{-1}M^{-1}$ in the presence of 30% methanol. Error was relatively large, particularly at methanol concentrations of 10% and 15% by volume, however the observed trends appear to be consistent when accounting for error (Figure 9).

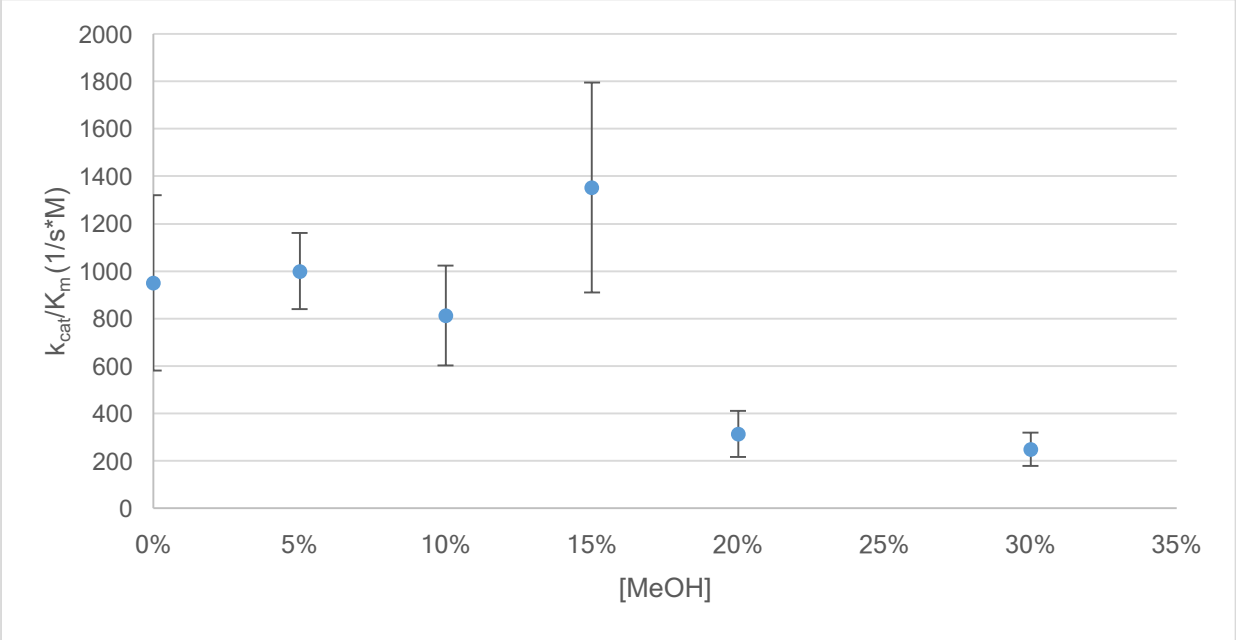

Figure 8: Effect of methanol on catalytic efficiency of Rv0045c.
A fluorogenic kinetic assay was used to analyze the catalytic efficiency of Rv0045c. The average of three replicate reaction rates of the hydrolysis of MOAME was plotted against [MOAME] in Origin 6.1 software to produce a hyperbola to fit standard Michaelis-Menten kinetics. K_m and k_{cat} were calculated and used to determine the catalytic efficiency of the enzyme. Increasing methanol concentrations appears to decrease the catalytic efficiency of the enzyme.

Ethanol

The presence of ethanol affected Rv0045c thermal stability in a manner very similar to methanol. The T_m was depressed to 30°C at 20% methanol by volume (Figure 8). As explained previously, completion of assays on different days likely led to slight variation in results, resulting in an unsmooth curve of the trend. Again, no viable data could be obtained at concentrations greater than 30% due to the inability to detect a change in fluorescence in an environment of that hydrophobicity.

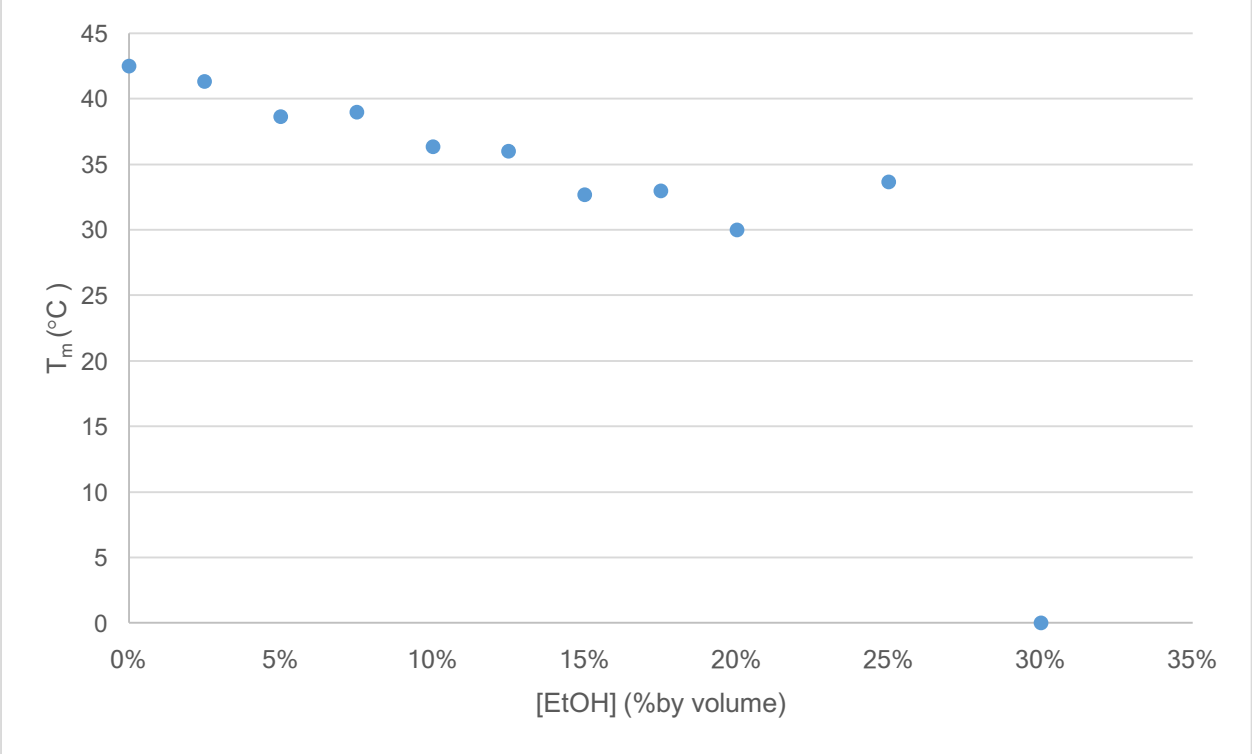

Figure 9: Presence of ethanol decreases the thermal stability of Rv0045c

Differential scanning fluorimetry (DSF) with SYPRO orange was used to determine the "melting point" of Rv0045c. Melting points shown are the average of three replicates. Increasing concentrations of ethanol yielded a steady decrease in thermal stability of the enzyme melting point could not be determined at [EtOH] > 30% due to limitations of the instrument to detect a change in fluorescence in a highly hydrophobic system.

Consistent with the effect of methanol concentration, ethanol seems to increase the k_{cat}/K_m of Rv0045c from 0% to 10% ethanol, with 10% having the highest such value,

at 4022 $s^{-1}M^{-1}$. The activity then decreases with increasing ethanol concentration to a k_{cat}/K_m of 859.3 $s^{-1}M^{-1}$ at 30% ethanol (Figure 9). There is no data for 25% ethanol as the instrument malfunctioned during the assay. The similarities in trend to methanol made the need for this data minimal, so the assay was not repeated.

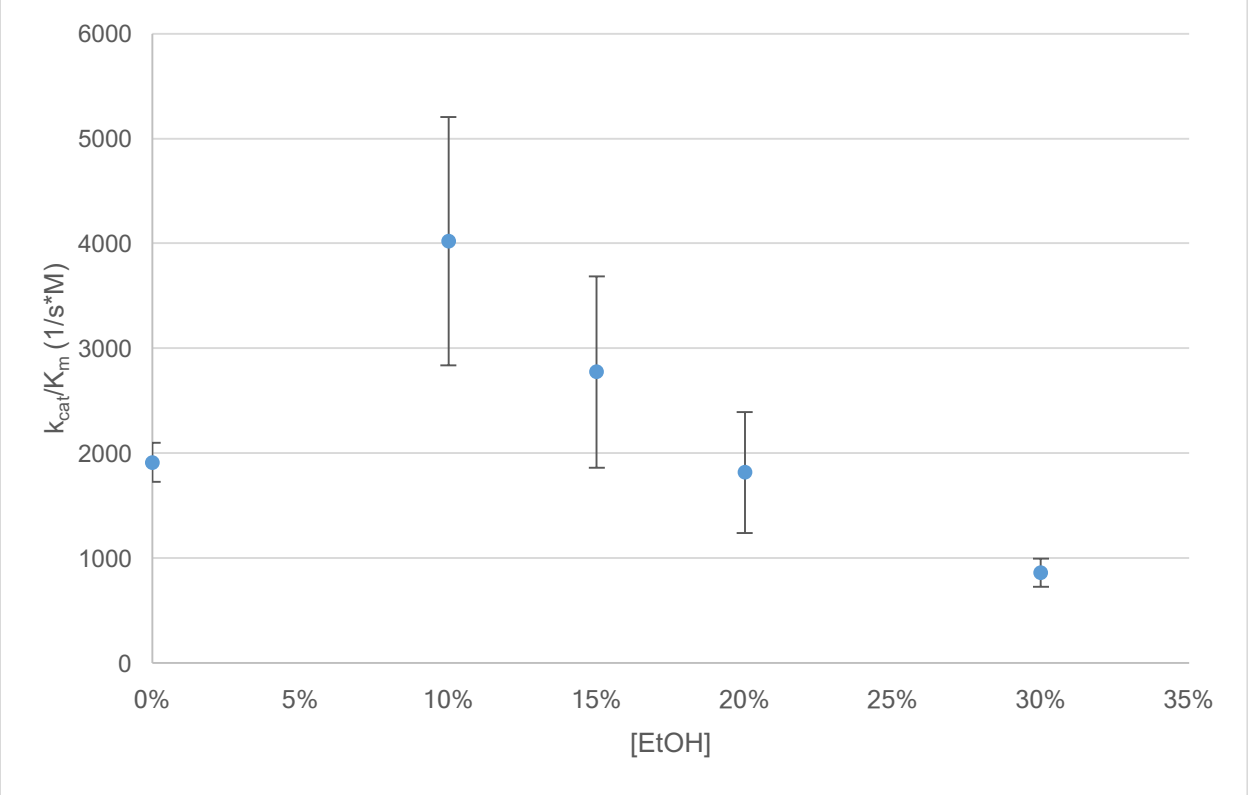

Figure 10: Effect of ethanol on catalytic efficiency of Rv0045c.

A fluorogenic kinetic assay was used to analyze the catalytic efficiency of Rv0045c. The average of three replicate reaction rates of the hydrolysis of MOAME was plotted against [MOAME] in origin 6.1 software to produce a hyperbola to fit standard Michaelis-Menten kinetics. K_m and k_{cat} were calculated and used to determine the catalytic efficiency of the enzyme. Increasing ethanol concentrations, once greater than 10% by volume appears to decrease the catalytic efficiency of the enzyme.

Isopropanol

Fewer data points were collected for thermal stability of Rv0045c in the presence of increasing concentrations of isopropanol, as previous assays with other alcohols indicated that trends would still be evident with larger intervals between data points.

Similarly to methanol and ethanol, isopropanol concentration depressed the melting point of Rv0045c, from 42°C when no alcohol was present, to 27°C at 20% isopropanol (Figure 10). Data shown for 30% isopropanol is likely inaccurate, as only a single data point arose from running the assay in triplicate. Analysis was not completed at concentrations greater than 30% isopropanol since no valuable data was collected in previous experiments at similar concentrations. It is possible that the same problems with hydrophobicity and overwhelming of the system at fault for no reliable data above concentrations of 30% alcohol is to blame for the lack of accurate data for 30% isopropanol.

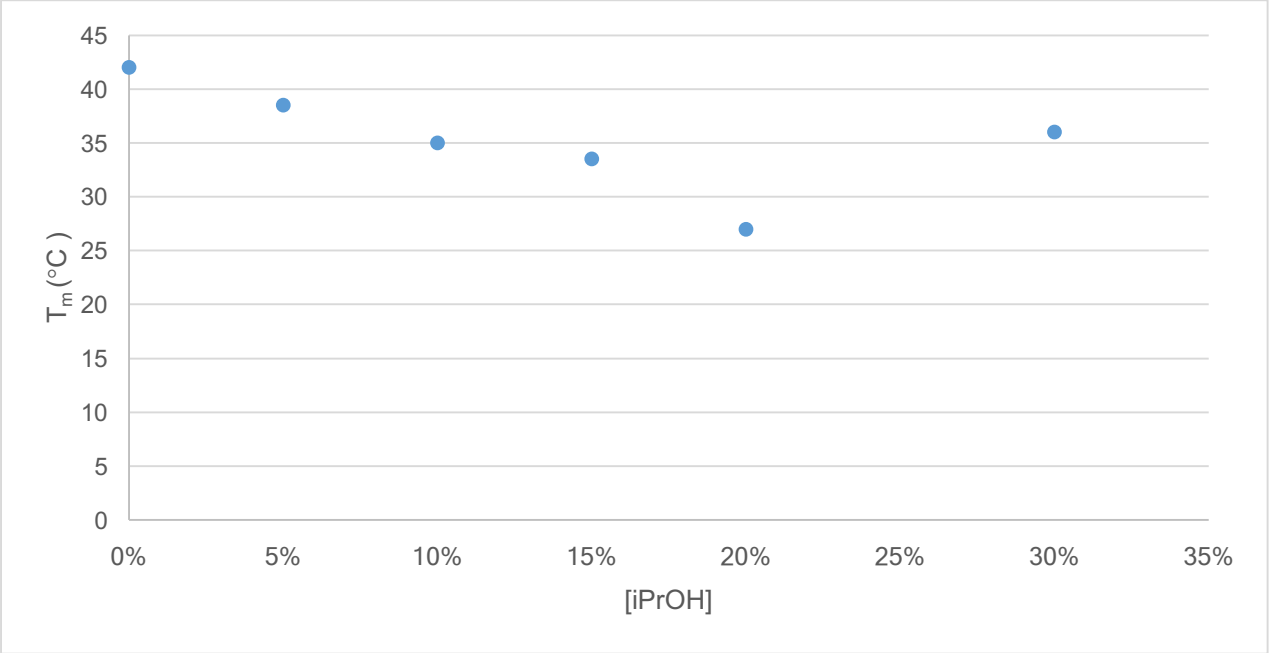

Figure 11: Presence of isopropanol decreases the thermal stability of Rv0045c.

Differential scanning fluorimetry (DSF) with SYPRO orange was used to determine the "melting point" of Rv0045c. Melting points shown are the average of three replicates. Increasing concentrations of isopropanol yielded a steady decrease in thermal stability of the enzyme. Melting point could not be determined at [iPrOH] > 30% due to limitations of the instrument to detect a change in fluorescence in a highly hydrophobic system.

Kinetic analysis of Rv0045c in the presence of isopropanol yielded results highly similar to that in the presence of methanol or ethanol. The highest $k_{cat}/K_{m,}$ which was equal to 1034 $s^{-1}M^{-1}$ was observed at 10% isopropanol and then generally decreased with concentration to a value of 245.9 $s^{-1}M^{-1}$ at 25% isopropanol (Figure 11). As noted previously, the error associated with these values was particularly high at 10% and 20% isopropanol, but the observed trend remains largely unchanged even when accounting for error.

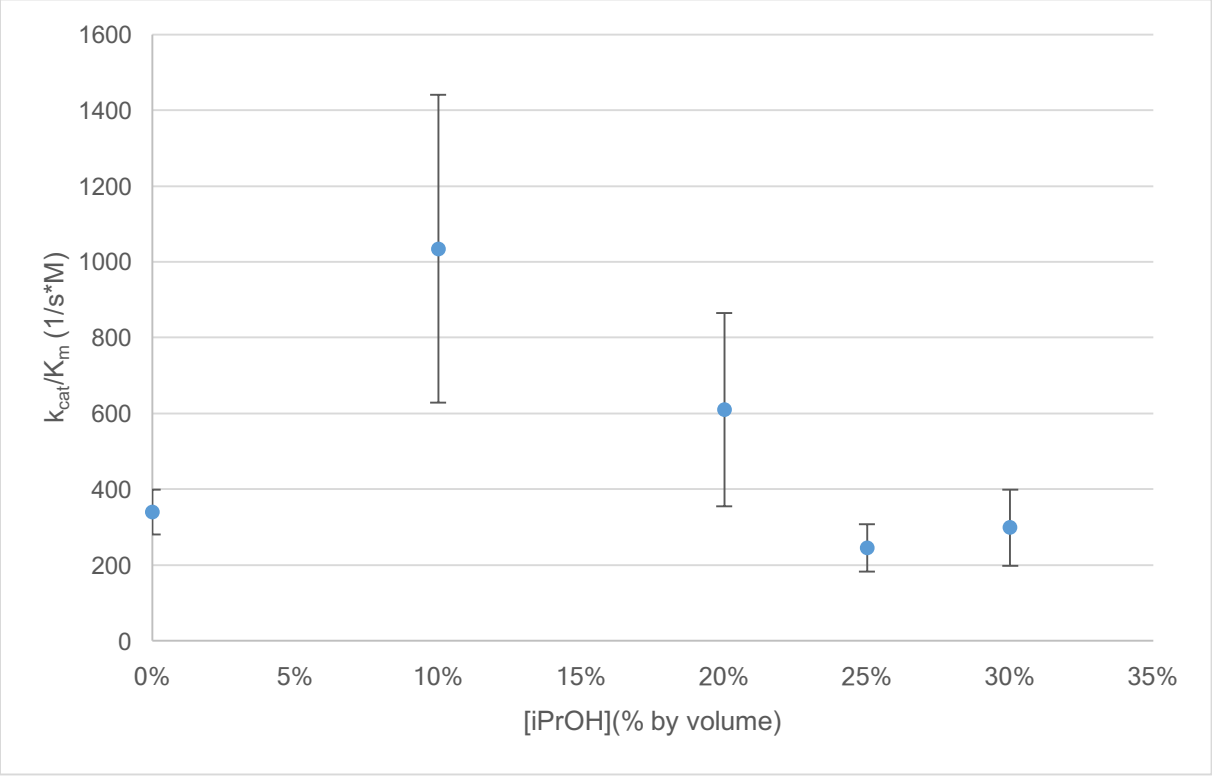

Figure 12: Effect of isopropanol on catalytic efficiency of Rv0045c.

A fluorogenic kinetic assay was used to analyze the catalytic efficiency of Rv0045c. The average of three replicate reaction rates of the hydrolysis of MOAME was plotted against [MOAME] in origin 6.1 software to produce a hyperbola to fit standard Michaelis-Menten kinetics. K_m and k_{cat} were calculated and used to determine the catalytic efficiency of the enzyme. Increasing isopropanol concentrations, once greater than 10% by volume appears to decrease the catalytic efficiency of the enzyme.

Unpublished data collected by students at Butler University in 2013 gave rise to the idea that the addition of monoalcohols to wild type Rv0045c may lead to an increase in catalytic activity. These results indicated that there is likely an optimal catalytic efficiency achieved near 10-15% alcohol by volume which became clear when results for each alcohol were analyzed together rather than individually. Similar to the trend observed with glycerol, it appears as if optimal activity occurs at 10% alcohol in the presence of ethanol or isopropanol by volume. Optimal activity when in the presence of methanol occurred at 15%, though it is likely that large error contributed to this difference and the data may not be entirely reliable. It appears as though there is no correlation between stability and activity, as stability of Rv0045c decreased rather steadily in the presence of methanol, ethanol, or isopropanol. It is possible that this is due to increased substrate solubility in the presence of low concentrations of alcohol. The hydrophobic nature of the alcohols may surround individual molecules of substrate in a way which more easily transports them to the active site of Rv0045c. This would account for increases in activity due to a decrease in K_m without having to consider minor decreases in stability of the enzyme.

Thermal Stability Error and Limitations

While thermal stability results were relatively consistent, a somewhat large amount of error presents itself when analyzing data for each of the four alcohols collectively rather than individually. Each assay was completed in triplicate though the instrument was relatively limited in that temperatures were only programmed and recorded in integer increments, resulting in data lacking in precision. A recorded difference in T_m between trials of 1°C may be a response to a smaller change in

temperature than is evident. Errors of this nature are likely responsible for the differences in the measured T_m of Rv0045c in the absence of alcohol from one assay to the next. Additionally, data points of T_m collected in the same instrumental analysis generally followed the same trend line, though data from different analyses appear to have somewhat unsteady trend lines, resulting in the slightly unsteady trend lines observed for Rv0045c in the presence of methanol or ethanol.

Though the small errors mentioned above may contribute to the observed results slightly, the biggest impact on results arises from the relatively small range of the instrument for detecting changes in fluorescence. As noted previously, thermal stability could not be determined at concentrations above 30% alcohol by volume for alcohols with a destabilizing effect (methanol, ethanol, and isopropanol). The extremely hydrophobic environment created by these alcohols allows for fluorescence to be relatively high to begin with and the system is easily overwhelmed when attempting to detect changes at such high values. This meant that no usable data could be collected above concentrations of 30% alcohol by volume in trials involving methanol, ethanol, or isopropanol. Additionally, concentrations at or approaching this limit often resulted in at least one failed replicate for which no data was collected, decreasing the reliability of the data.

Kinetic Assay Error and Limitations

In addition to error likely affecting the thermal stability results presented here, the k_{cat}, K_m and k_{cat}/K_m are also adversely affected by relatively high error values. Many of the error values resulting from the fluorogenic kinetic assays are an entire order of magnitude larger than is considered acceptable. This is likely due to a recurring issue in data

analysis when creating hyperbolas to fit Michaelis-Menten kinetics. In many of these plots, the data point corresponding to a substrate concentration of 100 μM has a lower rate (y-value) than the previous data point at a concentration of 50 μM. This is abnormal in that the curve should be approaching a maximum value, not decreasing. This discrepancy is likely not the fault of the true kinetic behavior of the enzyme, but rather is due to systematic error of the assay. However, the effect of this on the relative differences between these kinetic measures is likely negligible as the error is somewhat consistent.

Conclusions and Future Direction

Rv0045c in the presence of glycerol led to interesting results in that thermal stability can be increased while activity levels remain generally unchanged. Previous research has shown that glycerol acts in a protective manner for storing proteins [16] and thus a likely application of these results is the use of glycerol in PBS rather than PBS alone to store Rv0045c for use in future assays. This could allow for an elongated amount of time that Rv0045c could be used after purification and could potentially allow for the purified protein to be stored at temperatures below 0°C without affecting the activity levels of the protein. Aside from results surrounding glycerol, it is interesting to note that there appears to be an optimal alcohol concentration for maximizing catalytic activity of Rv0045c. This trend was not further investigated, though understanding the cause or causes of this trend may allow for further understanding of the mechanism through which Rv0045c acts. It is possible that a more dynamic structure observed with lower T_m in the presence of alcohols is related to the observed increase in k_{cat}/K_m and more specifically the observed decrease in K_m. Increased flexibility of the structure may allow for the substrate to reach the active site more easily.

A significant amount of further research could be completed to further the understanding of the findings presented here, as well as to continue exploring other factors which may influence Rv0045c stability and activity levels. Further investigation of the optimal alcohol concentration for Rv0045c activity levels is important to determine why such a phenomenon would occur and if such knowledge can be utilized to better understand Rv0045c as an individual protein or *M. tuberculosis* as an entire organism. Additionally, further studies should be completed to determine the ideal glycerol

concentration for storage of Rv0045c. Results should indicate a concentration which both maximizes stability under various temperature conditions and minimizes deviation in catalytic activity from that of the wild type enzyme in the absence of alcohol.

References

1. Centers for Disease Control and Prevention. Tuberculosis: Data and Statistics. http://www.cdc.gov/tb/statistics/

2. National Institutes of Allergy and infectious Diseases. Tuberculosis Cause. http://www.niaid.nih.gov/topics/tuberculosis/Understanding/Pages/cause.aspx

3. Cole ST; Brosch R; Parkhill J; Garnier T; Churcher D; et al. Deciphering the biology of *Mycobaterium tuberculosis* from the complete genome sequence. *Nature*. **1998.** 393, 537-544.

4. Guo J; Zheng X; Xu L; Zhongyuan L; Xu K; et al. Characterization of a Novel Esterase Rv0045c from *Mycobacterium tuberculosis*. *PLoS ONE*. **2010.** 5(10).

5. Bachovchin DA and Cravatt BF. The pharmacological landscape and therapeutic potential of serine hydrolases. *Nature Reviews.* **2012.** 11. 52-68.

6. Zheng X; Guo J; Xu L; Honglei L; Dongwei Z; et al. Crystal Structure of a Novel Esterase Rv0045c from *Mycobacterium tuberculosis*. *PLoS ONE.* **2011.** 6(5).

7. Lukowski JK; Savas CP; Gehring AM; McKary MG; Adkins CT; et al. Distinct Substrate Selectivity of a Metabolic Hydrolase from *Mycobacterium tuberculosis. Biochemistry.* **2014.** 53, 7386-7395.

8. Ellis EE; Adkins CT; Galovska NM; Lavis LD; Johnson RJ. Decoupled Roles for the Atypical, Bifurcated Binding Pocket of the ybfF Hydrolase. *ChemBioChem.* **2013.** 14, 1134-1144.

9. Ding J; Gao M; Hou G; Liang K. Effect of Ethanol Accumulation on Porcine Interferon-α Production by *Pichia pastoris* and Activities of Key Enzymes in

Carbon Metabolism. *Applied Biochemistry and Biotechnology.* **2015.** 176, 1964-1974.

10. Tchigvintsev A; Tran H; Popovic A; Kovacic F; Brown G; et. al. The Environment Shapes Microbial Enzymes: Five Cold-Active and Salt-Resistant Carboxylesterases from Marine Metagenomes. *Applied Microbiology and Biotechnology.* **2015.** 99, 2165-2178.

11. Feng S and Yan YB. Effects of Glycerol on the Compaction and Stability of the Wild Type and Mutated Rabbit Muscle Creatine Kinase. *Proteins.* **2008.** 71, 844-854.

12. Johnson RJ; Savas CJ; Kartje Z; Hoops GC. Rapid and Adaptable Measurement of Protein Thermal Stability by Differential Scanning Fluorimetry: Updating a Common Biochemical Laboratory Experiment. *Journal of Chemical Education*. **2014.** 91, 1077-1080.

13. Niesen FH; Berglund H; Vedadi M. The use of differential scanning fluorimetry to detect ligand interactions that promote protein stability. *Nature Protocols.* **2007.** 2(9), 2212-2221.

14. Lavis LD and Raines RT. Bright Ideas for Chemical Biology, *ACS Chemical Biology*, **2008.** 3(3), 142-155.

15. Lavis LD; Chao T; Raines RT. Synthesis and utility of fluorogenic acetoxymethylesters. *The Royal Society of Chemistry.* **2010.**

16. Nakagawa Y; Sota M; Koumoto K. Cryoprotective Ability of Betaine-type Metabolic Analogs During Freezing Duration of Enzymes. *Biotechnology Letters.* **2015.** 37, 1607-1613.

Appendices

Appendix A: Differential Scanning Fluorimetry

Glycerol

[Glycerol]	T_m Trial 1 (°C)	T_m Trial 2 (°C)	T_m Trial 3 (°C)	Average T_m (°C)	Error
0%	42.00	42.00	42.00	42.00	0.00
2.50%	43.00	43.00	43.00	43.00	0.00
5%	44.00	45.00	44.00	44.33	0.58
7.50%	44.00	44.00	45.00	44.33	0.58
10%	45.00	45.00	45.00	45.00	0.00
12.50%	46.00	46.00	45.00	45.67	0.58
0%	43.00	43.00	43.00	43.00	0.00
7.50%	46.00	42.00	44.00	44.00	2.00
15%	46.00	46.00	46.00	46.00	0.00
22.50%	48.00	47.00	48.00	47.67	0.58
30%	49.00	49.00	48.00	48.67	0.58
37.50%	N/A	50.00	50.00	50.00	0.00
45%	51.00	51.00	51.00	51.00	0.00
57%	52.00	N/A	52.00	52.00	0.00

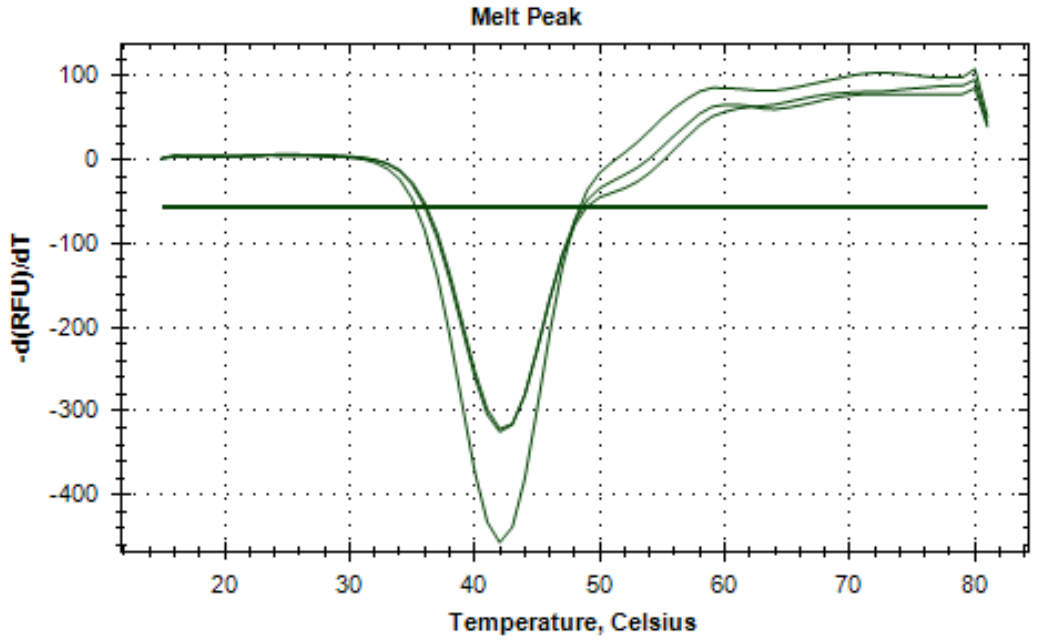

Rv0045c in the absence of glycerol

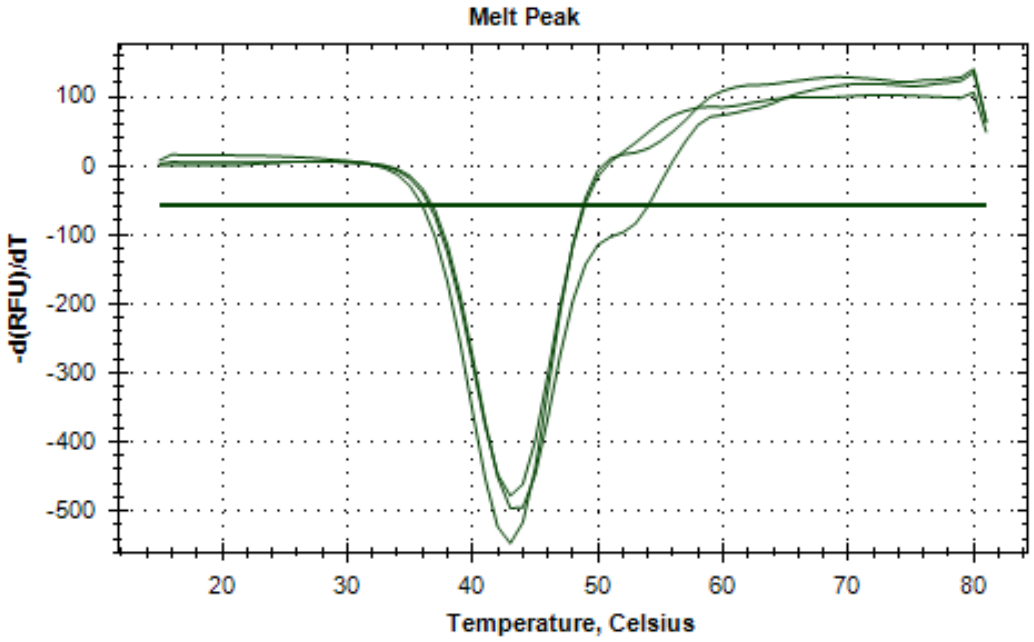

Rv0045c in the presence of 2.5% glycerol by volume

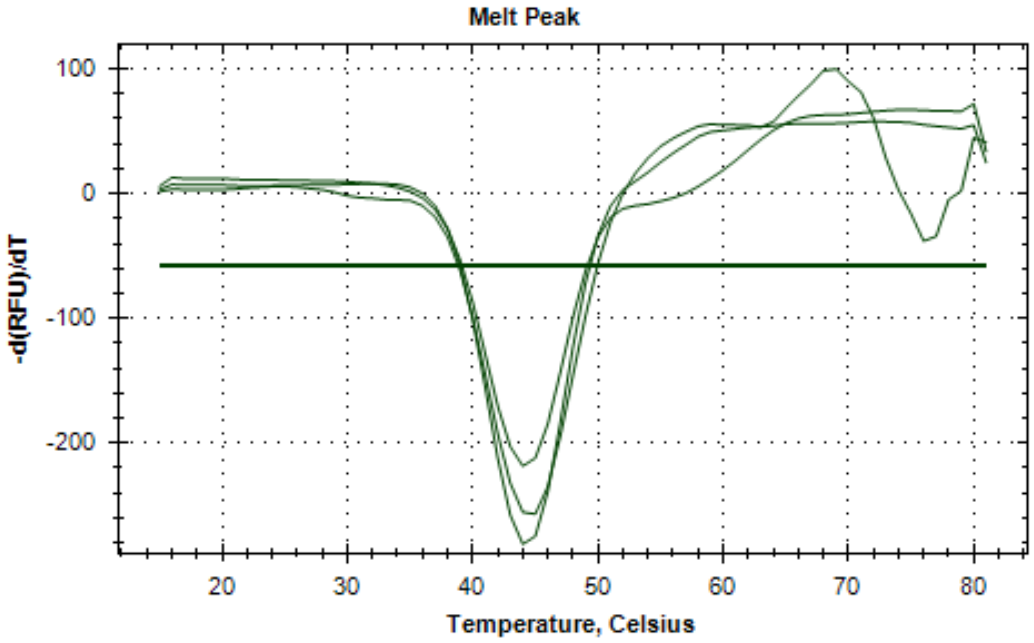

Rv0045c in the presence of 5% glycerol by volume

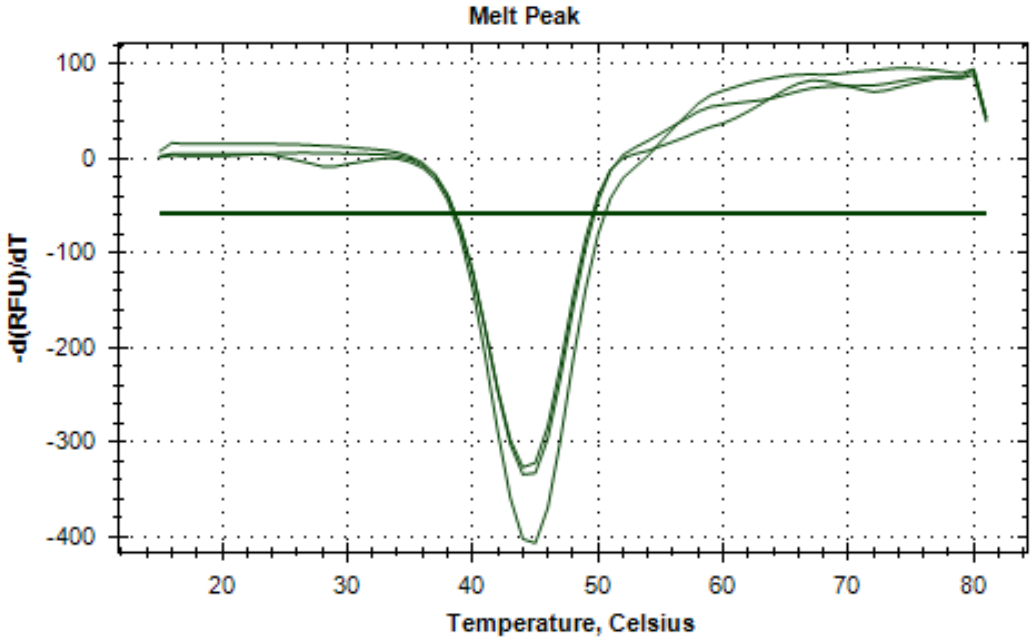

Rv0045c in the presence of 7.5% glycerol by volume

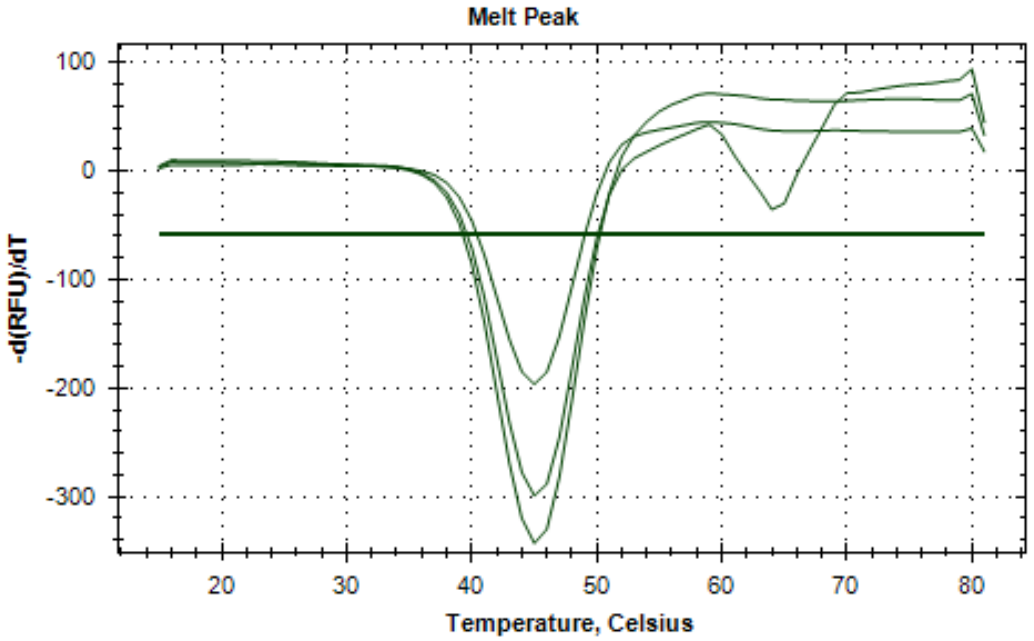

Rv0045c in the presence of 10% glycerol by volume

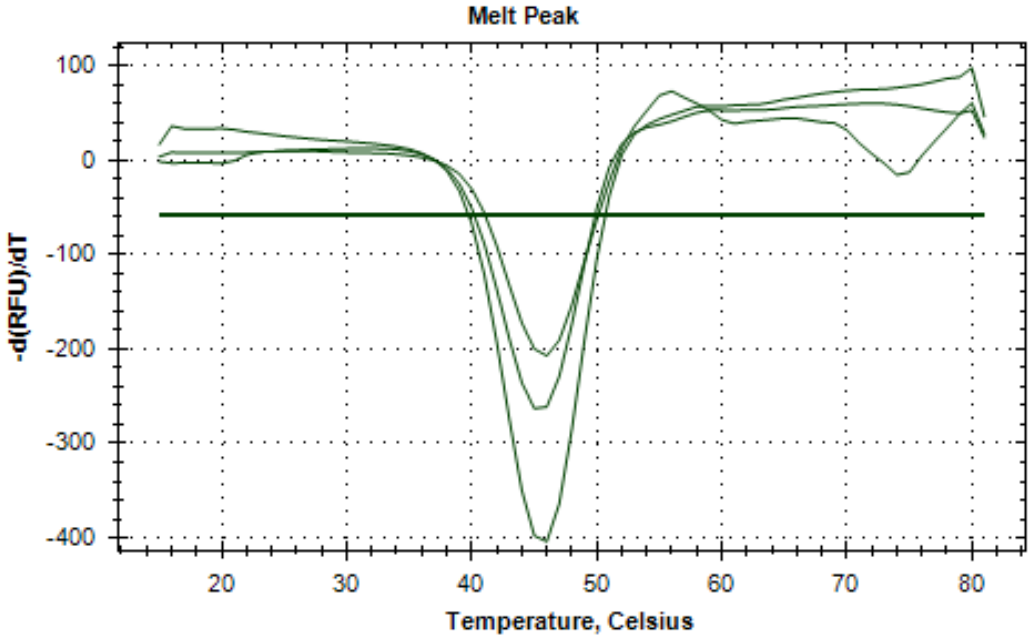

Rv0045c in the presence of 12.5% glycerol by volume

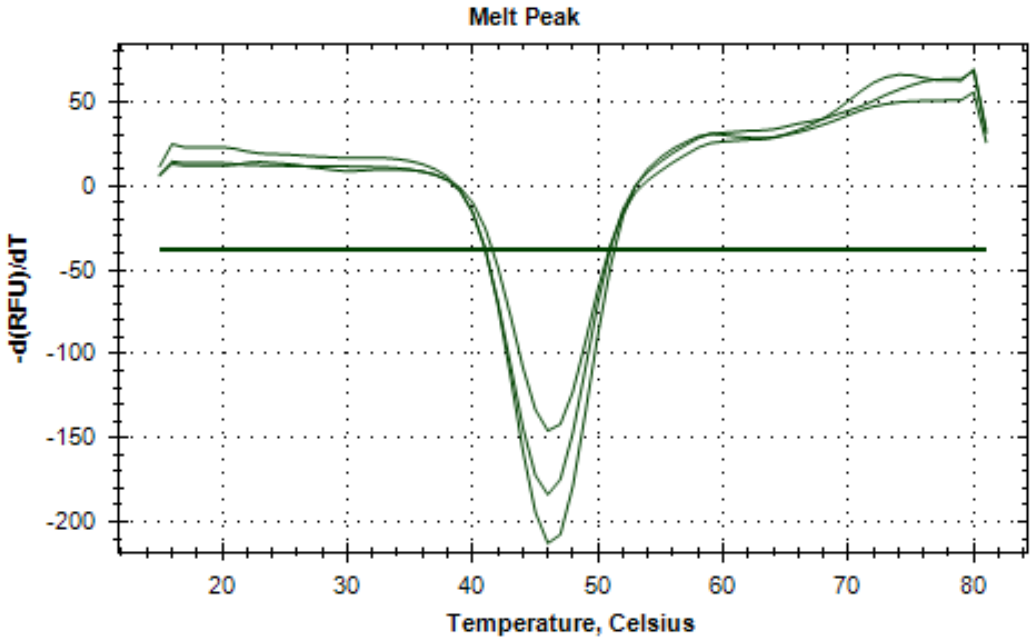

Rv0045c in the presence of 15% glycerol by volume

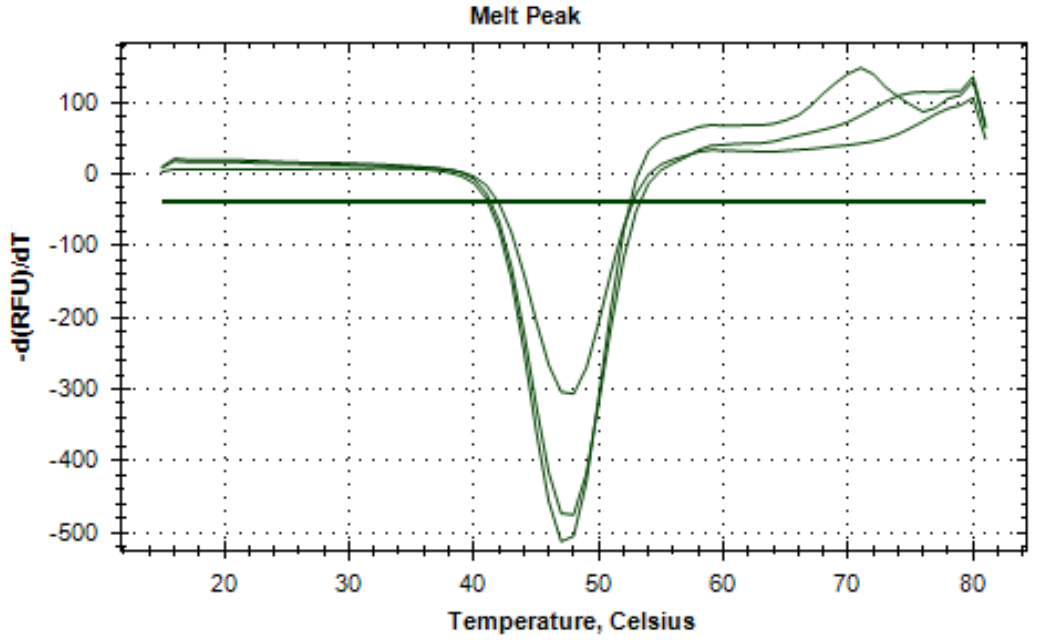

Rv0045c in the presence of 22.5% glycerol by volume

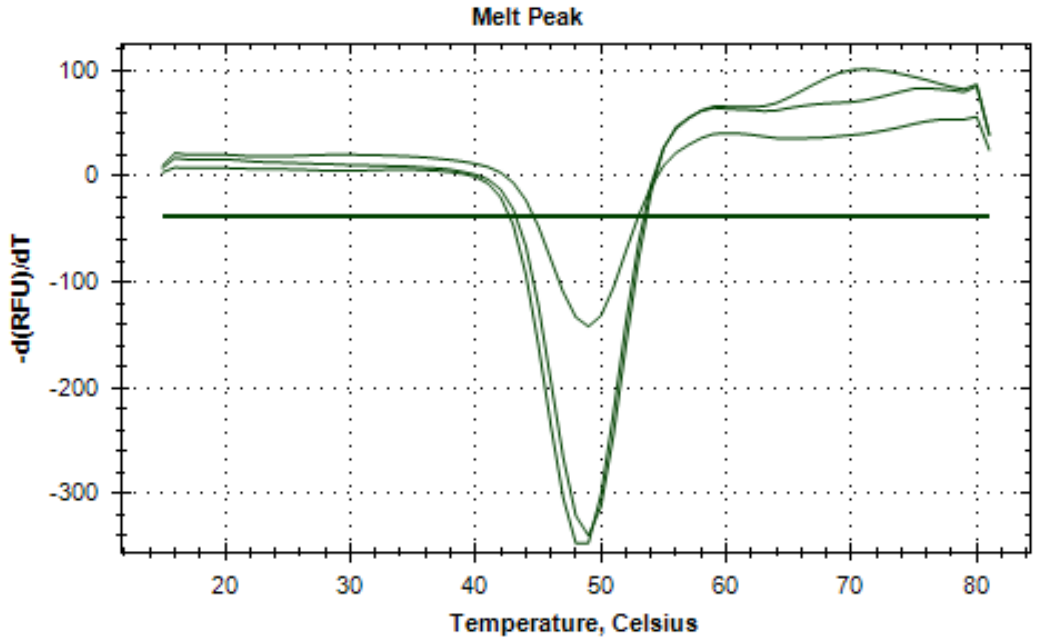

Rv0045c in the presence of 30% glycerol by volume

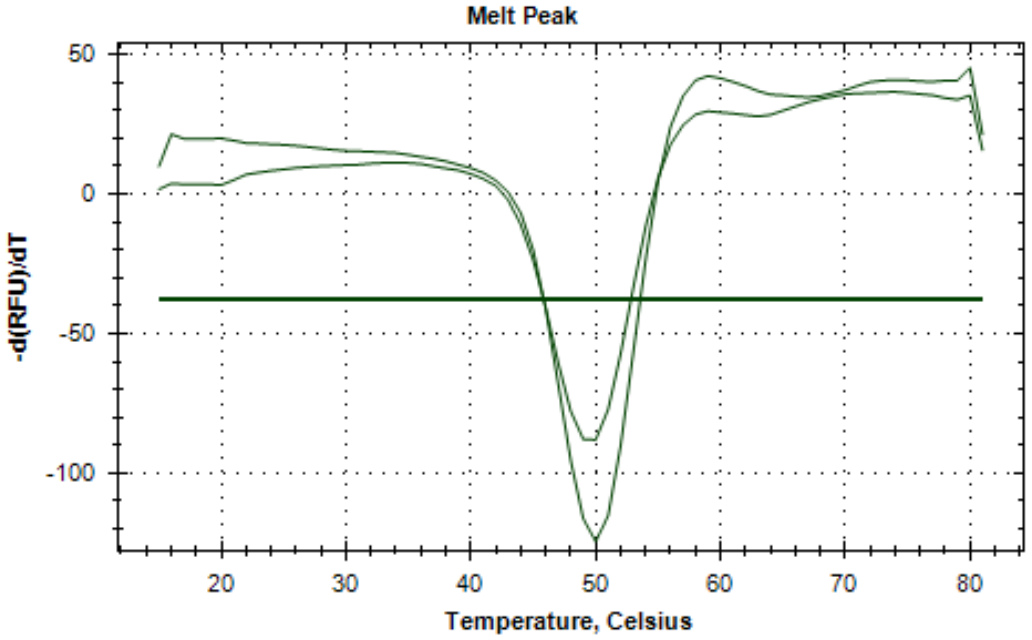

Rv0045c in the presence of 37.5% glycerol by volume

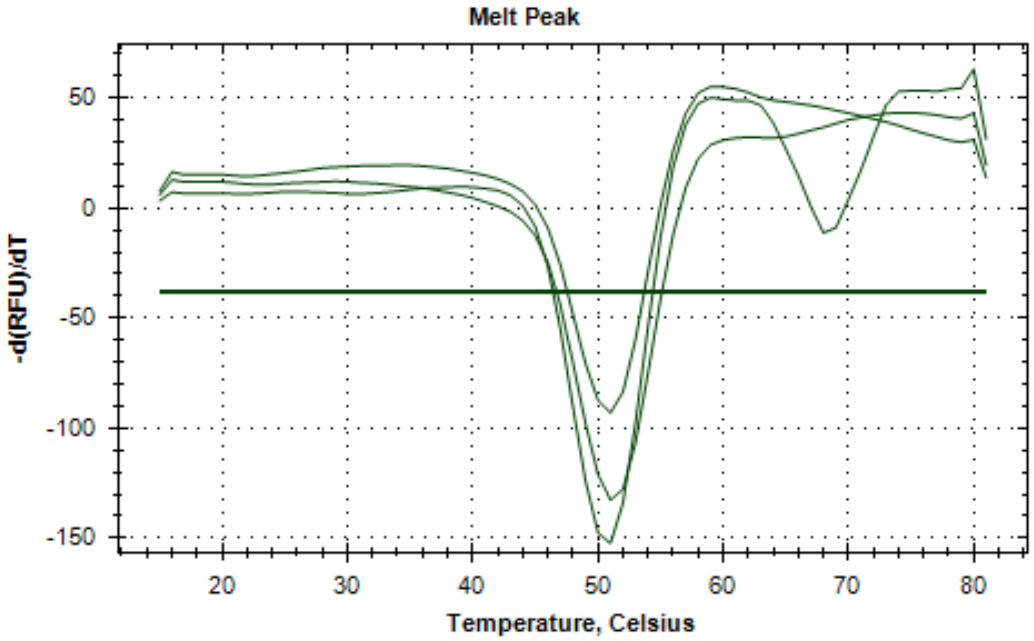

Rv0045c in the presence of 45% glycerol by volume

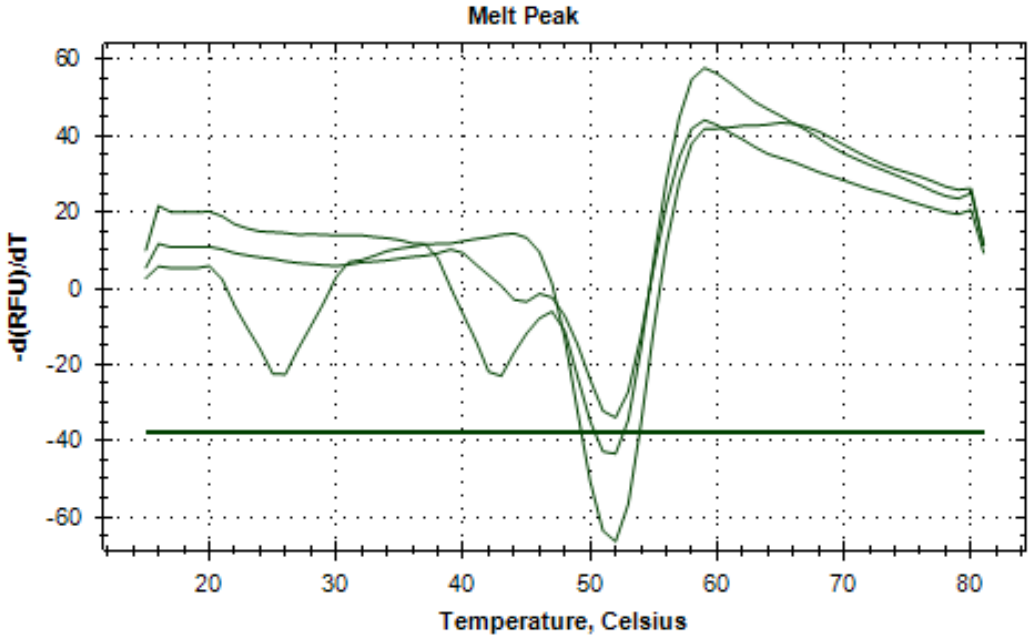

Rv0045c in the presence of 57% glycerol by volume

Methanol

[MeOH]	T_m Trial 1 (°C)	T_m Trial 2 (°C)	T_m Trial 3 (°C)	Average T_m (°C)	Error
0%	43.00	42.00	N/A	42.50	0.71
2.50%	42.00	42.00	42.00	42.00	0.00
5%	42.00	41.00	42.00	41.67	0.58
7.50%	41.00	41.00	41.00	41.00	0.00
10%	37.00	36.00	36.00	36.33	0.58
12.50%	40.00	40.00	40.00	40.00	0.00
15%	39.00	39.00	38.00	38.67	0.58
17.50%	37.00	37.00	37.00	37.00	0.00
20%	33.00	33.00	32.00	32.67	0.58
22.60%	33.00	33.00	33.00	33.00	0.00
25%	32.00	32.00	32.00	32.00	0.00
27.50%	29.00	29.00	29.00	29.00	0.00
30%	N/A	26.00	26.00	26.00	0.00
32.60%	N/A	N/A	31.00	31.00	17.90
35%	N/A	N/A	N/A	N/A	N/A

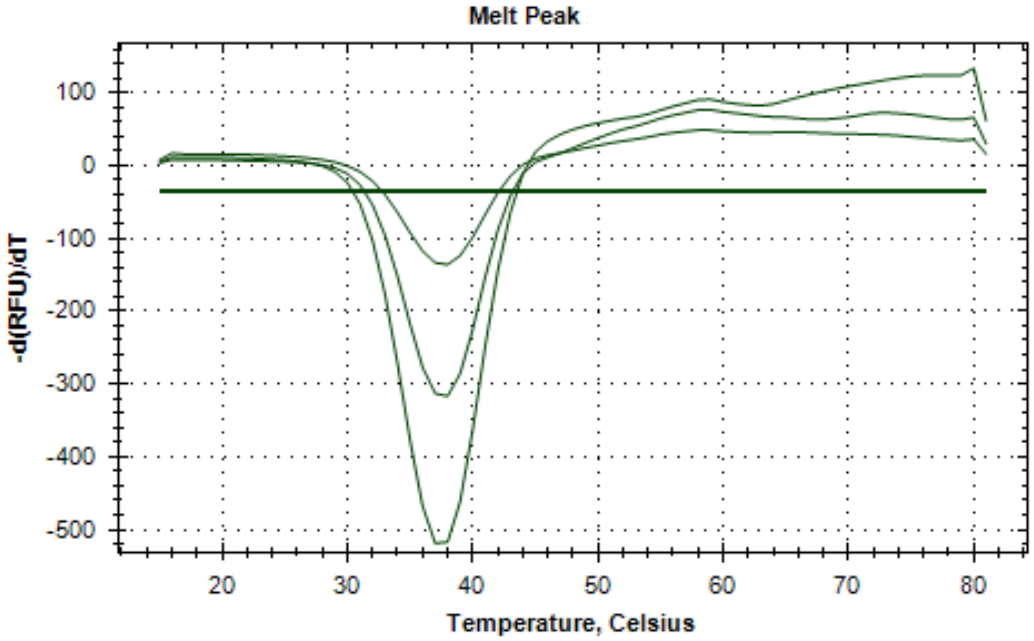

Rv0045c in the presence of 5% methanol by volume

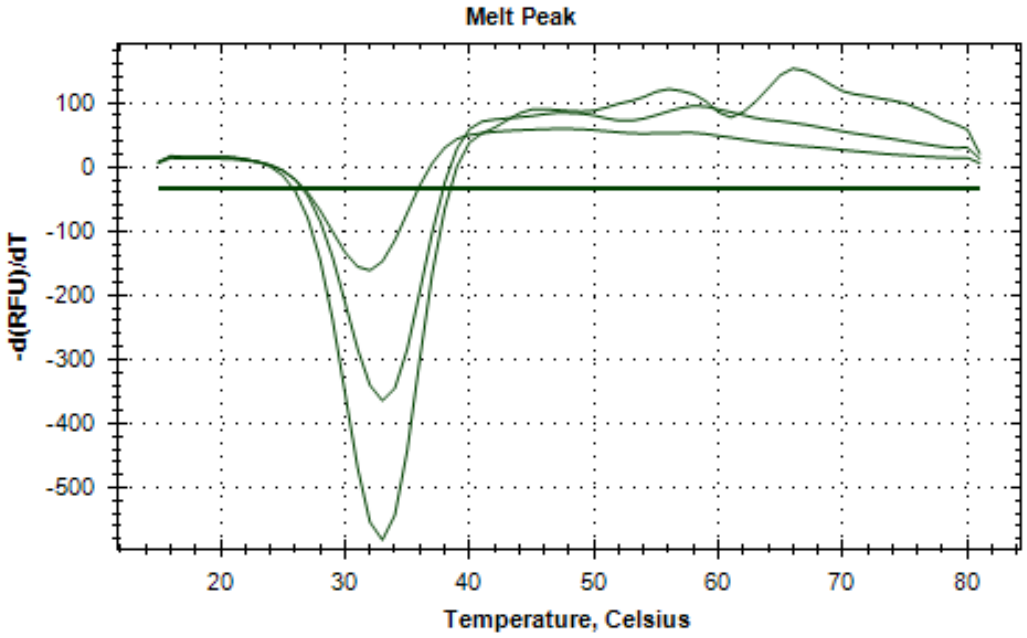

Rv0045c in the presence of 20% methanol by volume

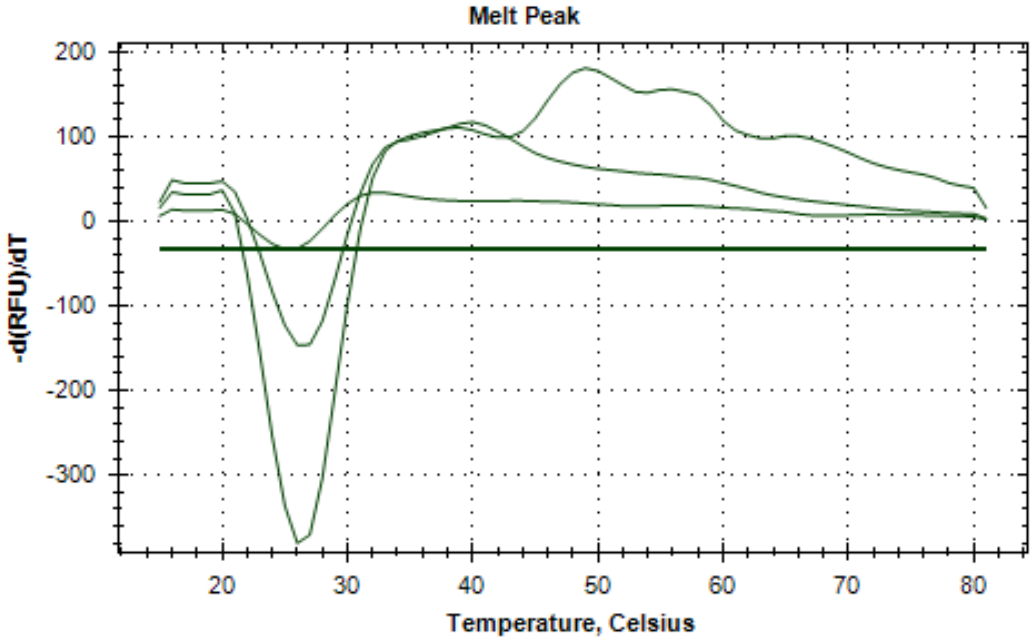

Rv0045c in the presence of 30% methanol

Ethanol

[EtOH]	T_m Trial 1 (°C)	T_m Trial 2 (°C)	T_m Trial 3 (°C)	Average T_m (°C)	Error
0%	43.00	42.00	N/A	42.50	0.71
2.50%	41.00	42.00	41.00	41.33	0.58
5%	38.00	39.00	39.00	38.67	0.58
7.50%	39.00	39.00	39.00	39.00	0.00
10%	36.00	36.00	37.00	36.33	0.58
12.50%	36.00	36.00	36.00	36.00	0.00
15%	33.00	33.00	32.00	32.67	0.58
17.50%	33.00	33.00	33.00	33.00	0.00
20%	30.00	30.00	N/A	30.00	0.00
25%	34.00	34.00	33.00	33.67	0.58
30%	N/A	N/A	N/A	N/A	N/A

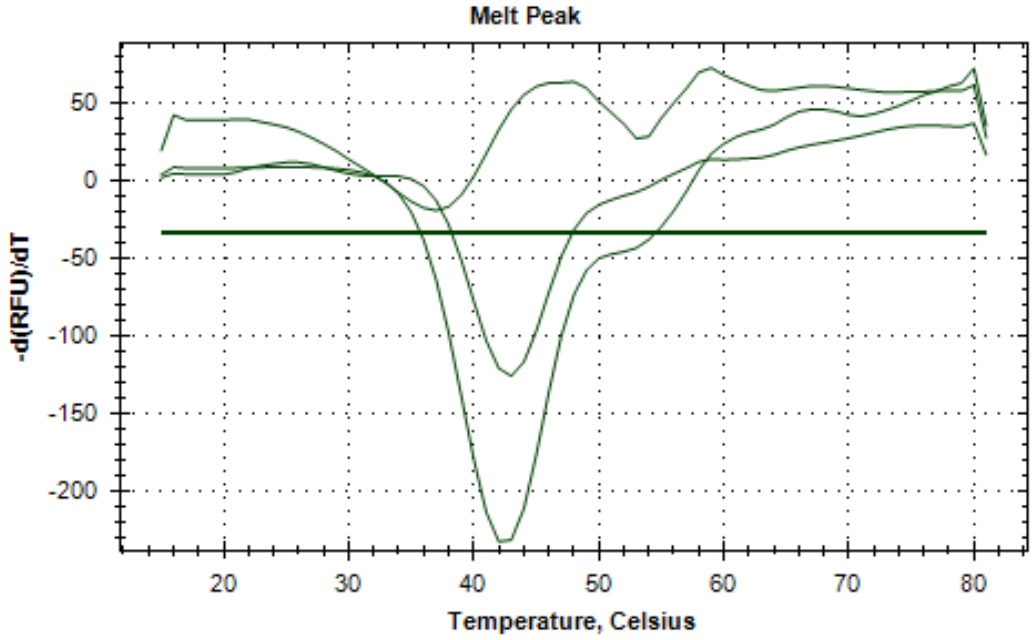

Rv0045c in the absence of ethanol

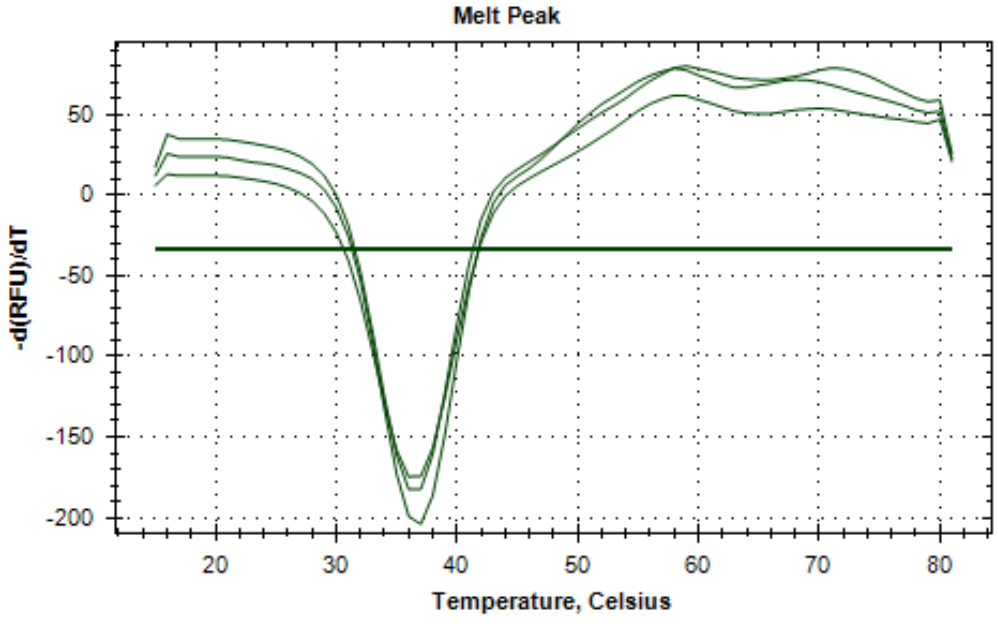

Rv0045c in the presence of 10% ethanol by volume

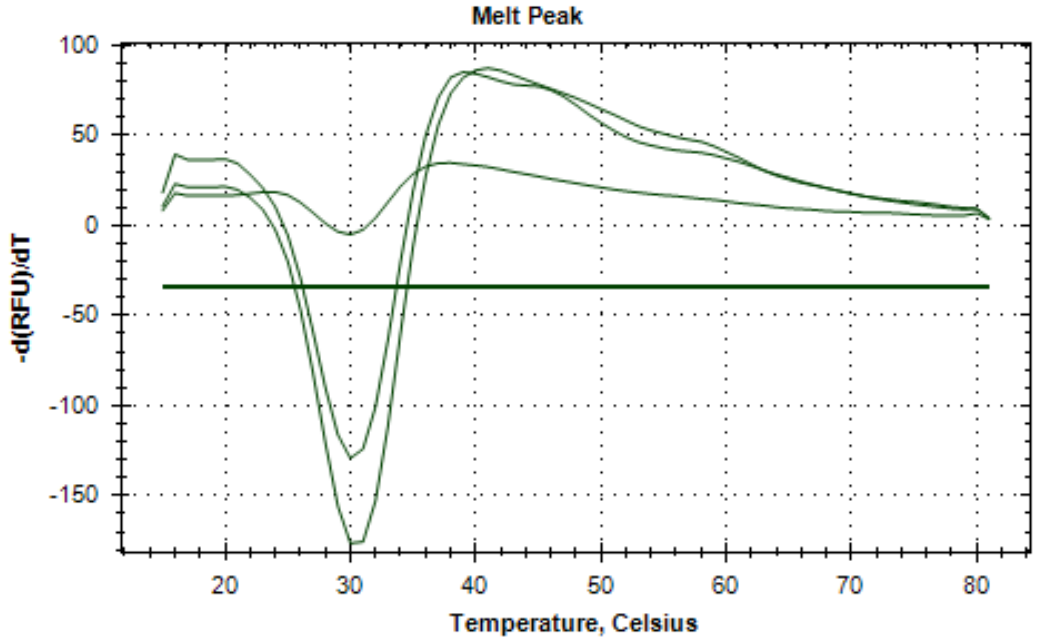

Rv0045c in the presence of 20% ethanol by volume

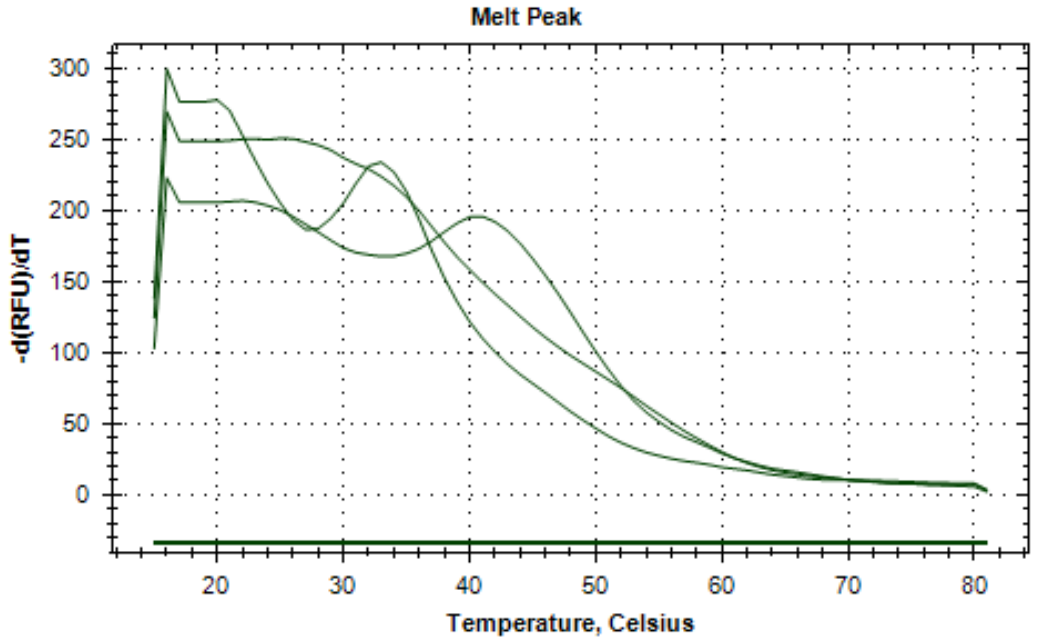

Rv0045c in the presence of 30% ethanol by volume

Isopropanol

[iPrOH]	T_m Trial 1 (°C)	T_m Trial 2 (°C)	T_m Trial 3 (°C)	Average T_m (°C)	Error
0%	42.00	42.00	42.00	42.00	0.00
5%	N/A	39.00	38.00	38.50	0.71
10%	34.00	35.00	36.00	35.00	1.00
15%	N/A	34.00	33.00	33.50	0.71
20%	N/A	N/A	27.00	27.00	0.00
30%	N/A	36.00	N/A	36.00	0.00

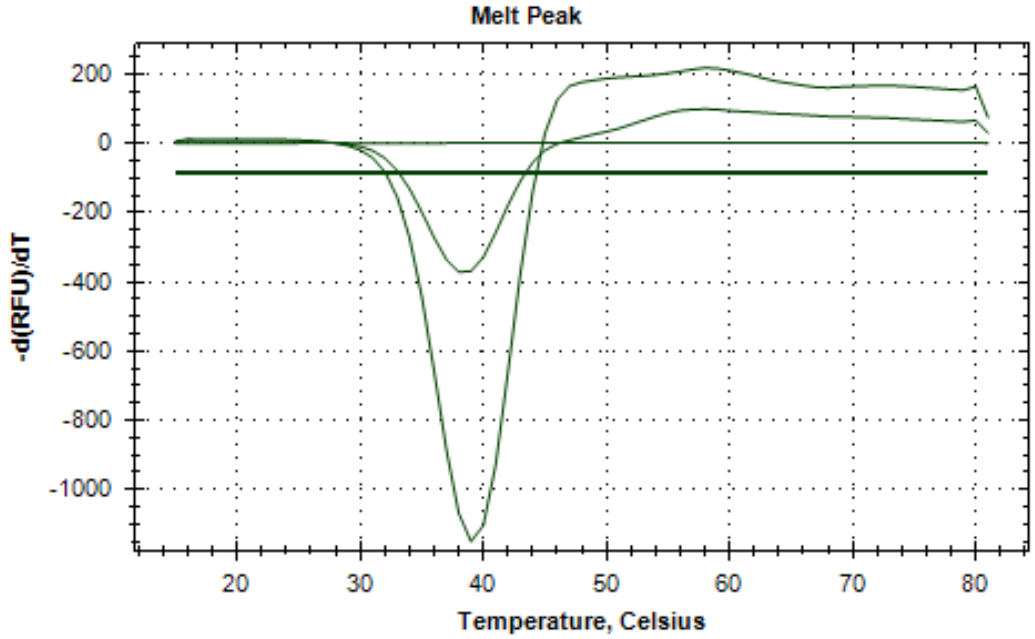

Rv0045c in the presence of 5% iPrOH by volume

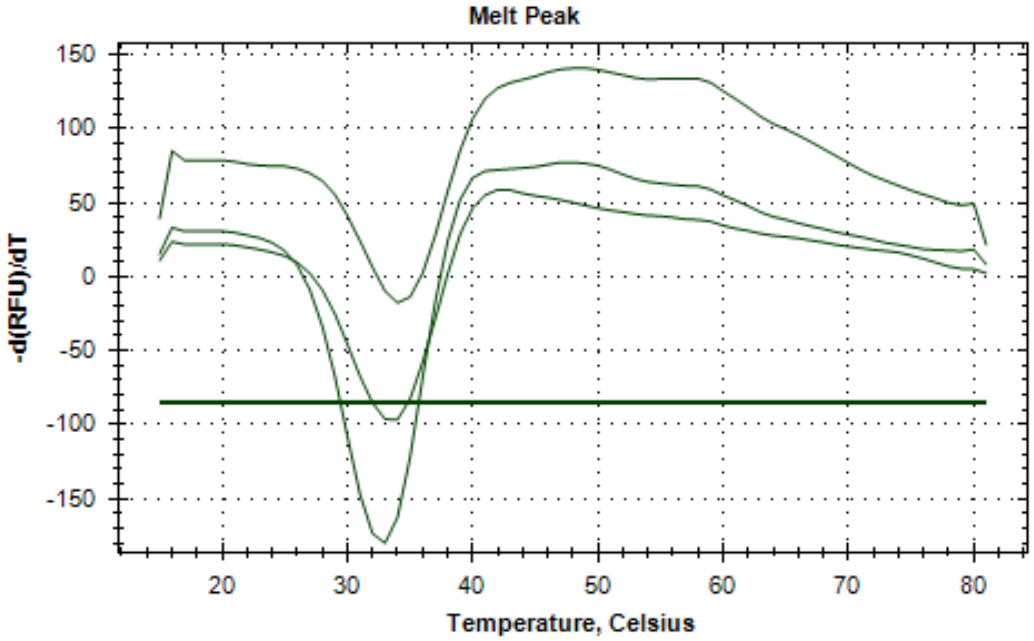

Rv0045c in the presence of 15% iPrOH by volume

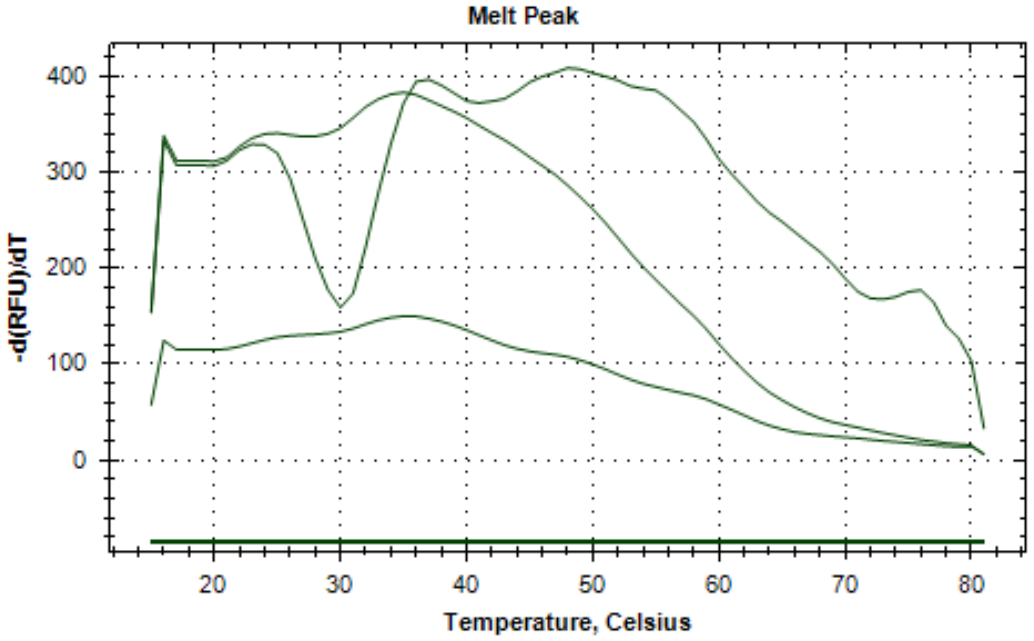

Rv0045c in the presence of 25% iPrOH by volume

Appendix B: Kinetics

Glycerol

[Glycerol]	k_{cat} (s^{-1})	k_{cat} error	K_m (μM)	K_m error	k_{cat}/K_m ($\mu M^{-1}s^{-1}$)	k_{cat}/K_m error
0%	0.00208	0.00014	7.42833	1.74233	0.00028	0.00007
5%	0.00164	0.00011	4.82781	1.27625	0.00034	0.00009
10%	0.00244	0.00021	4.77747	1.58033	0.00051	0.00017
15%	0.00096	0.00005	4.64479	0.92759	0.00021	0.00004
20%	0.00108	0.00009	11.64701	2.91062	0.00009	0.00002
25%	0.00152	0.00013	7.38348	2.15254	0.00021	0.00006

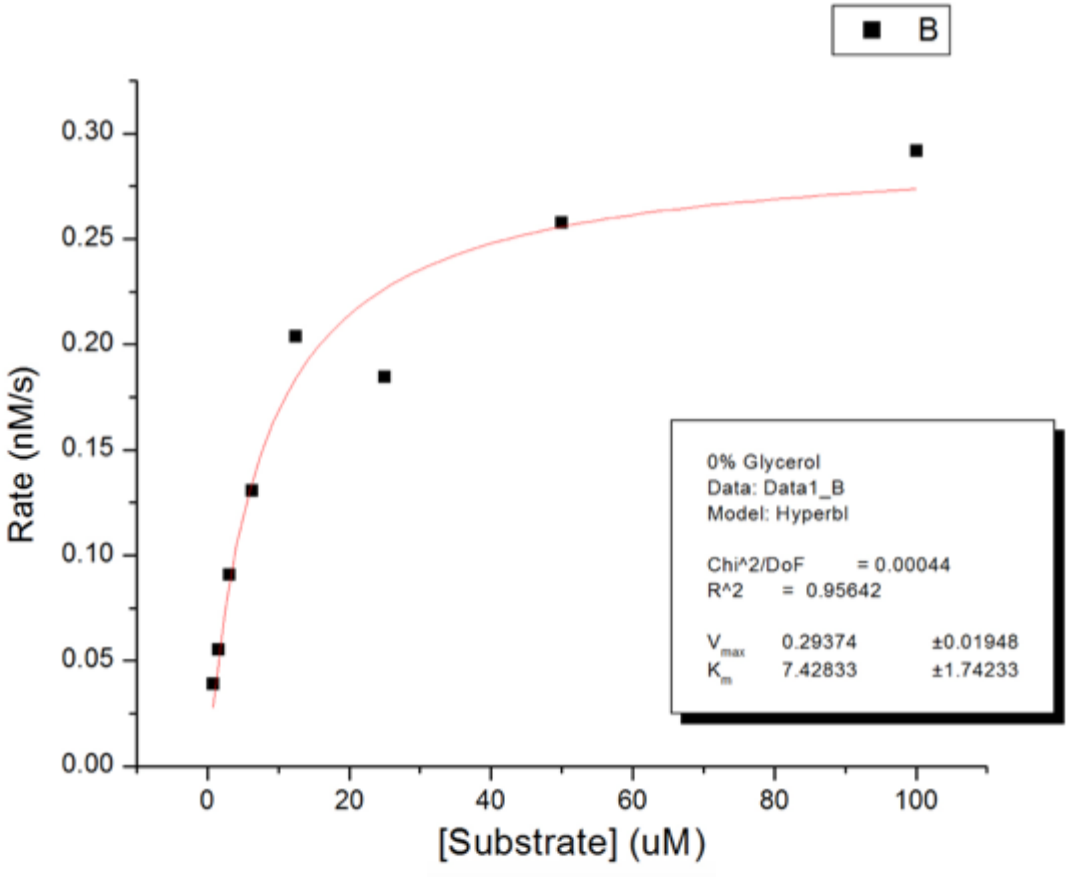

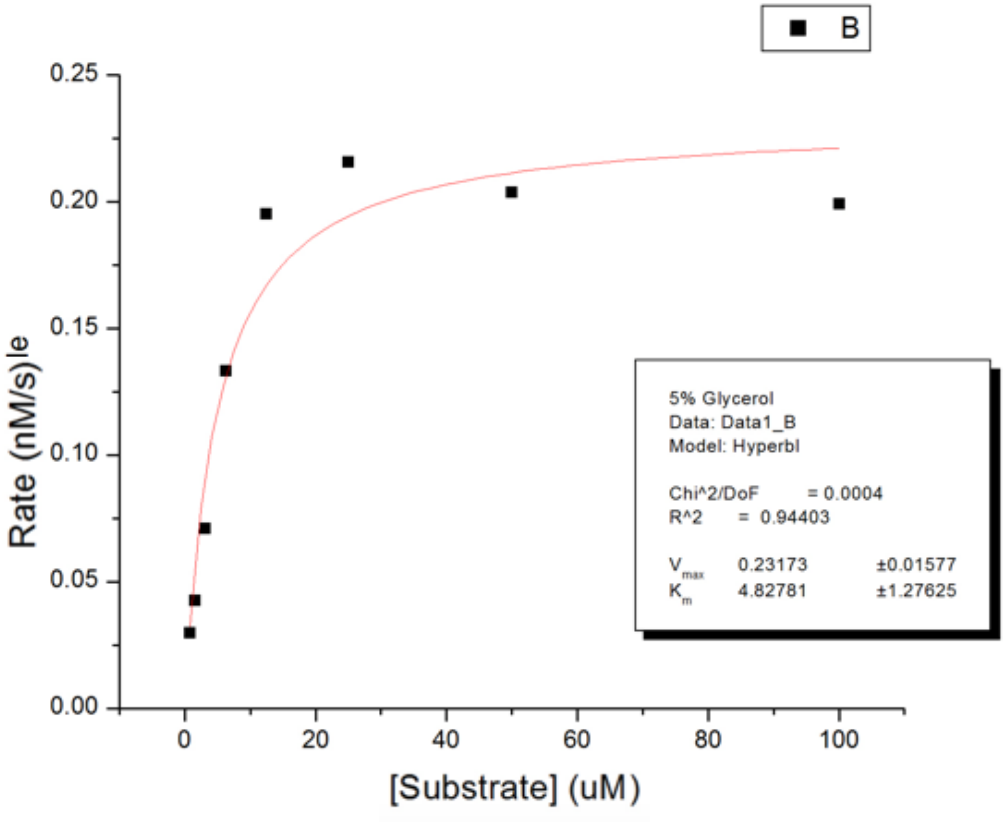
B
0.25
0.20
0.15
0.10
0.05
0.00
Rate (nM/s)le
0
20
40
60
80
100
[Substrate] (uM)
5% Glycerol
Data: Data1_B
Model: Hyperbl
Chi^2/DoF = 0.0004
R^2 = 0.94403
Vmax 0.23173 ±0.01577
Km 4.82781 ±1.27625

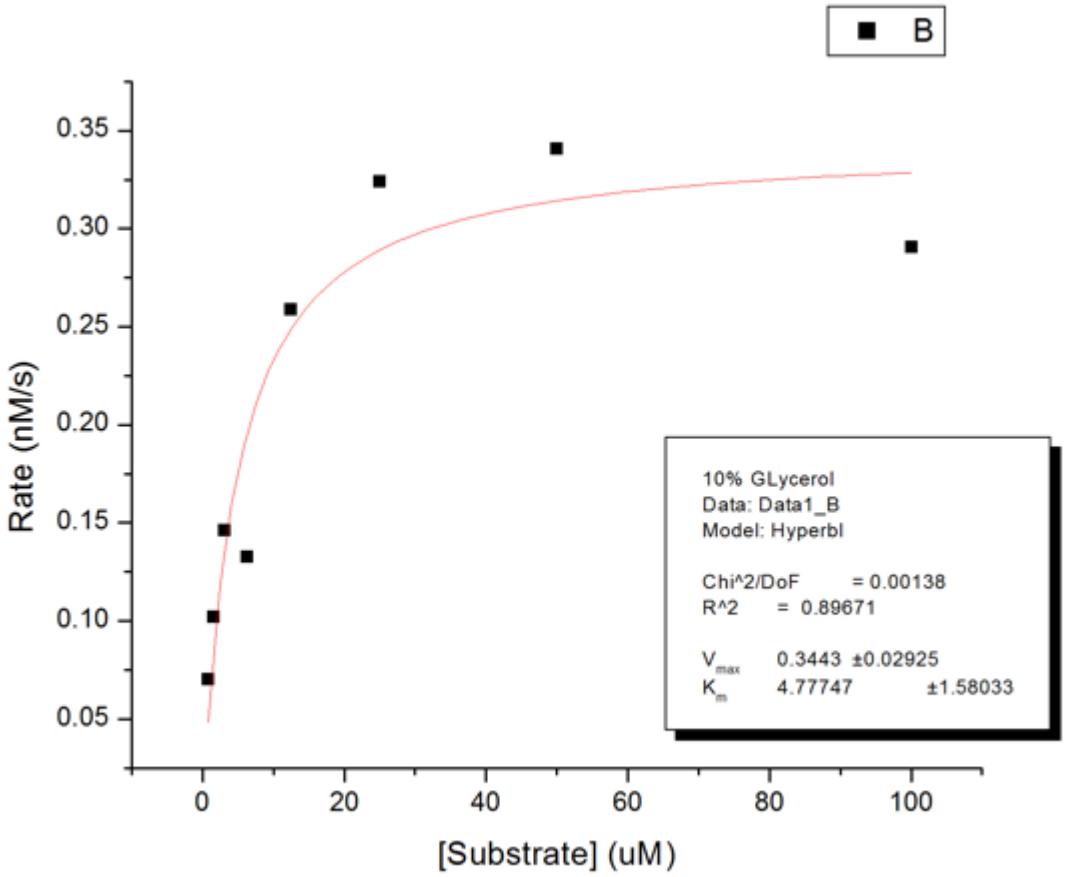
B
Rate (nM/s)
0.35
0.30
0.25
0.20
0.15
0.10
0.05
0
20
40
60
80
100
[Substrate] (uM)
10% GLycerol
Data: Data1_B
Model: Hyperbl
Chi^2/DoF = 0.00138
R^2 = 0.89671
V_max 0.3443 ±0.02925
K_m 4.77747 ±1.58033

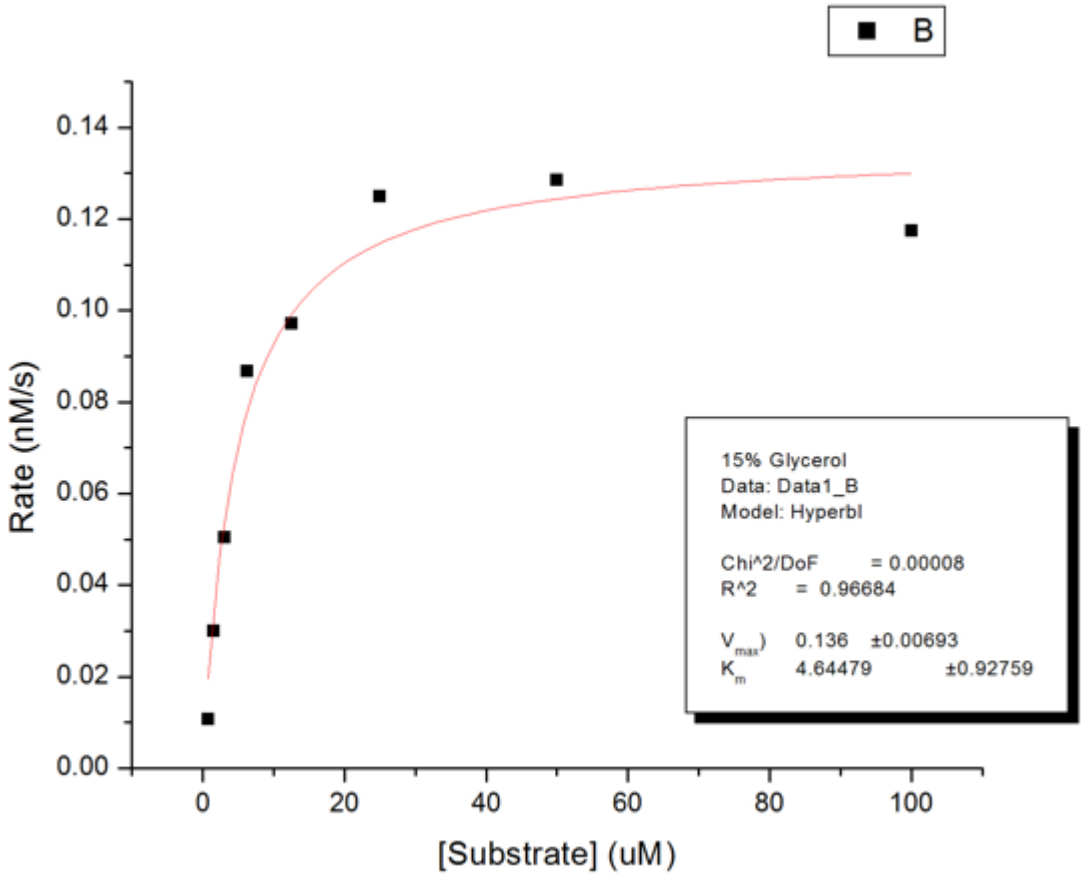
B
Rate (nM/s)
0.14
0.12
0.10
0.08
0.06
0.04
0.02
0.00
0
20
40
60
80
100
[Substrate] (uM)
15% Glycerol
Data: Data1_B
Model: Hyperbl
Chi^2/DoF = 0.00008
R^2 = 0.96684
V_max) 0.136 ±0.00693
K_m 4.64479 ±0.92759

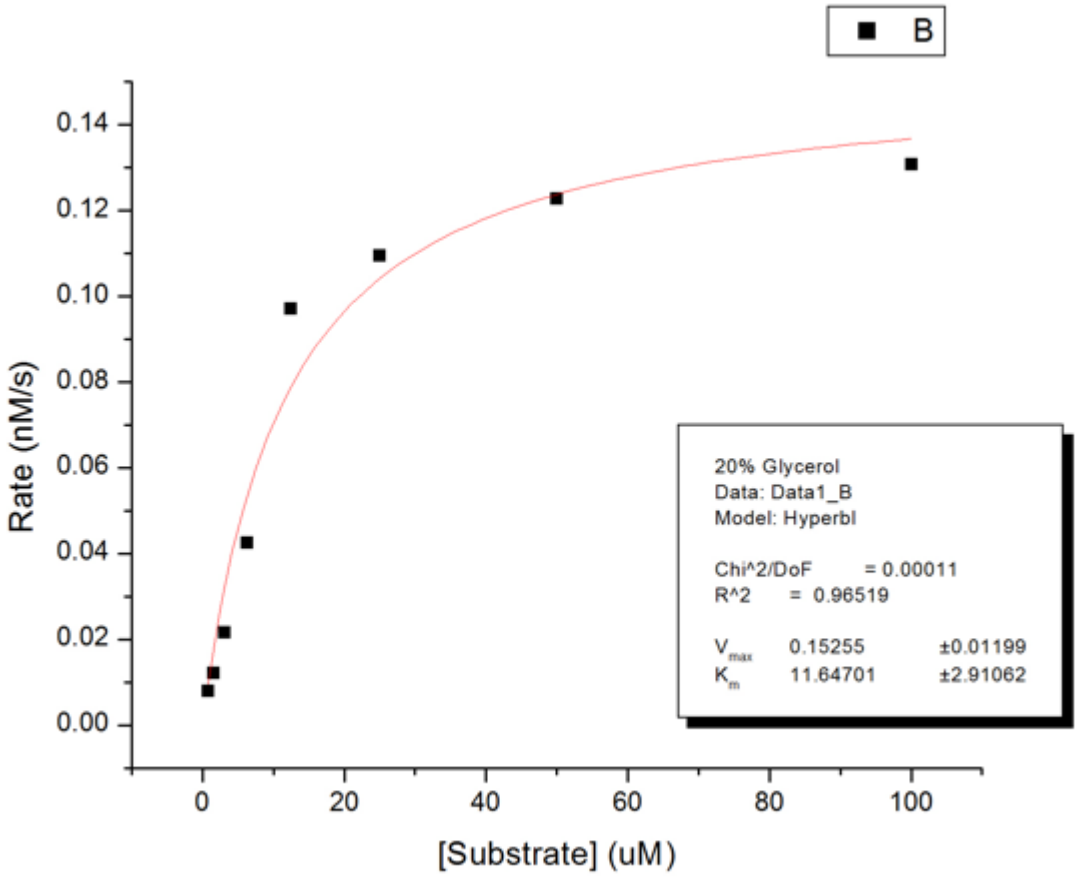
B
0.14
0.12
0.10
0.08
0.06
0.04
0.02
0.00
Rate (nM/s)
0
20
40
60
80
100
[Substrate] (uM)
20% Glycerol
Data: Data1_B
Model: Hyperbl
Chi^2/DoF = 0.00011
R^2 = 0.96519
Vmax 0.15255 ±0.01199
Km 11.64701 ±2.91062

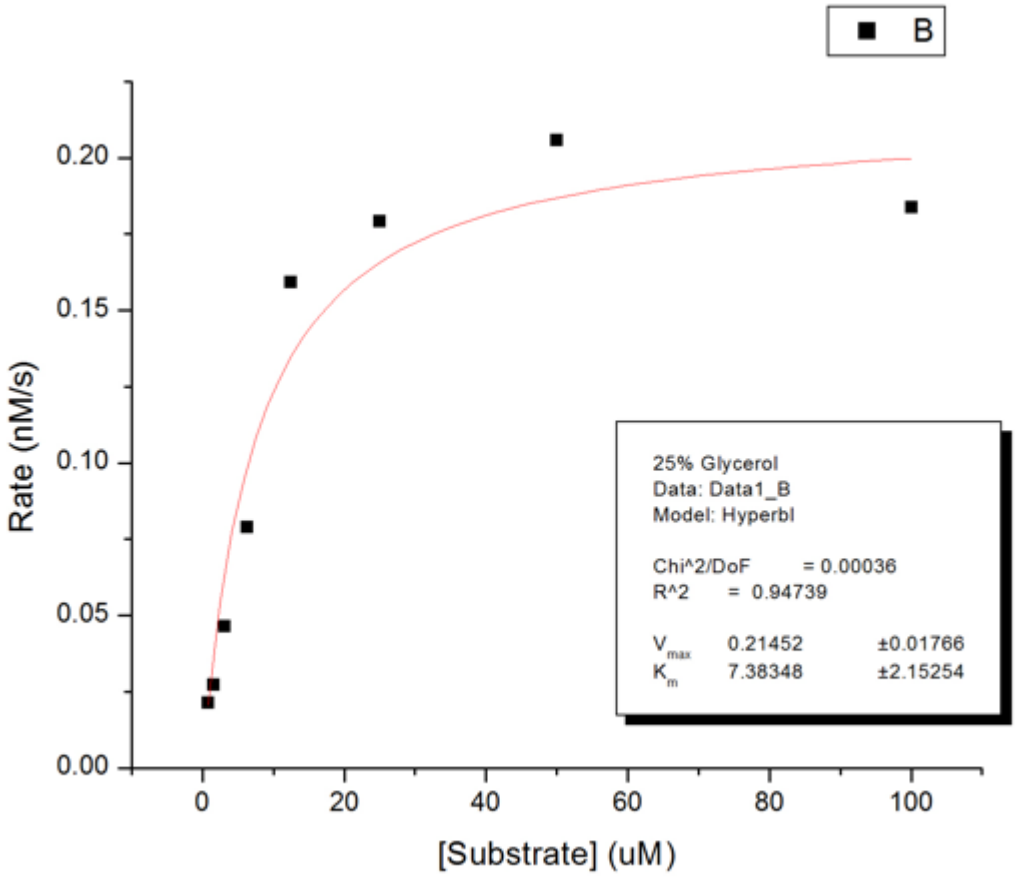

Methanol

[MeOH]	k_{cat} (s^{-1})	k_{cat} error	K_m (μM)	K_m error	k_{cat}/K_m ($\mu M^{-1}s^{-1}$)	k_{cat}/K_m error
0%	0.00997	0.00212	10.48645	3.42960	0.00095	0.00037
5%	0.00415	0.00016	4.14715	0.64372	0.00100	0.00016
10%	0.00291	0.00018	3.58279	0.89694	0.00081	0.00021
15%	0.00630	0.00051	4.65910	1.47966	0.00135	0.00044
20%	0.00539	0.00043	17.14406	5.12636	0.00031	0.00010
30%	0.00484	0.00036	19.38977	5.29999	0.00025	0.00007

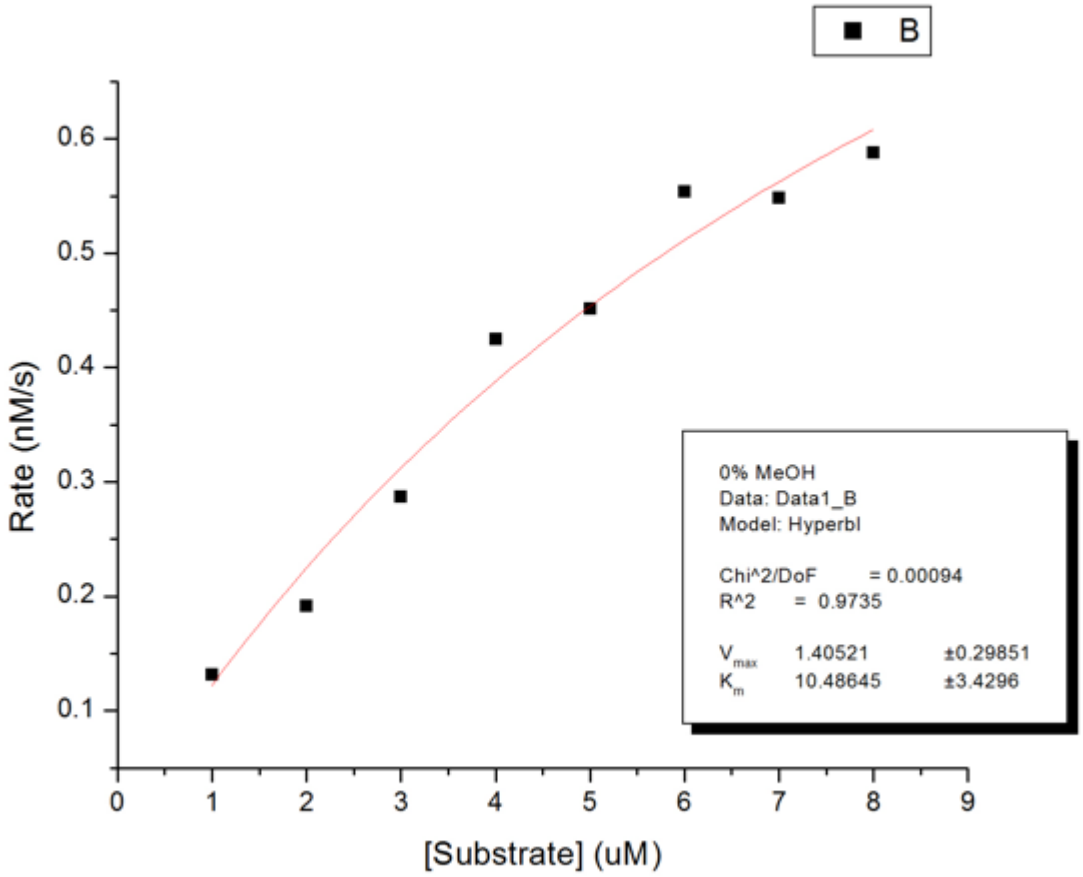
B
Rate (nM/s)
0.1
0.2
0.3
0.4
0.5
0.6
0
1
2
3
4
5
6
7
8
9
[Substrate] (uM)
0% MeOH
Data: Data1_B
Model: Hyperbl
Chi^2/DoF = 0.00094
R^2 = 0.9735
Vmax 1.40521 ±0.29851
Km 10.48645 ±3.4296

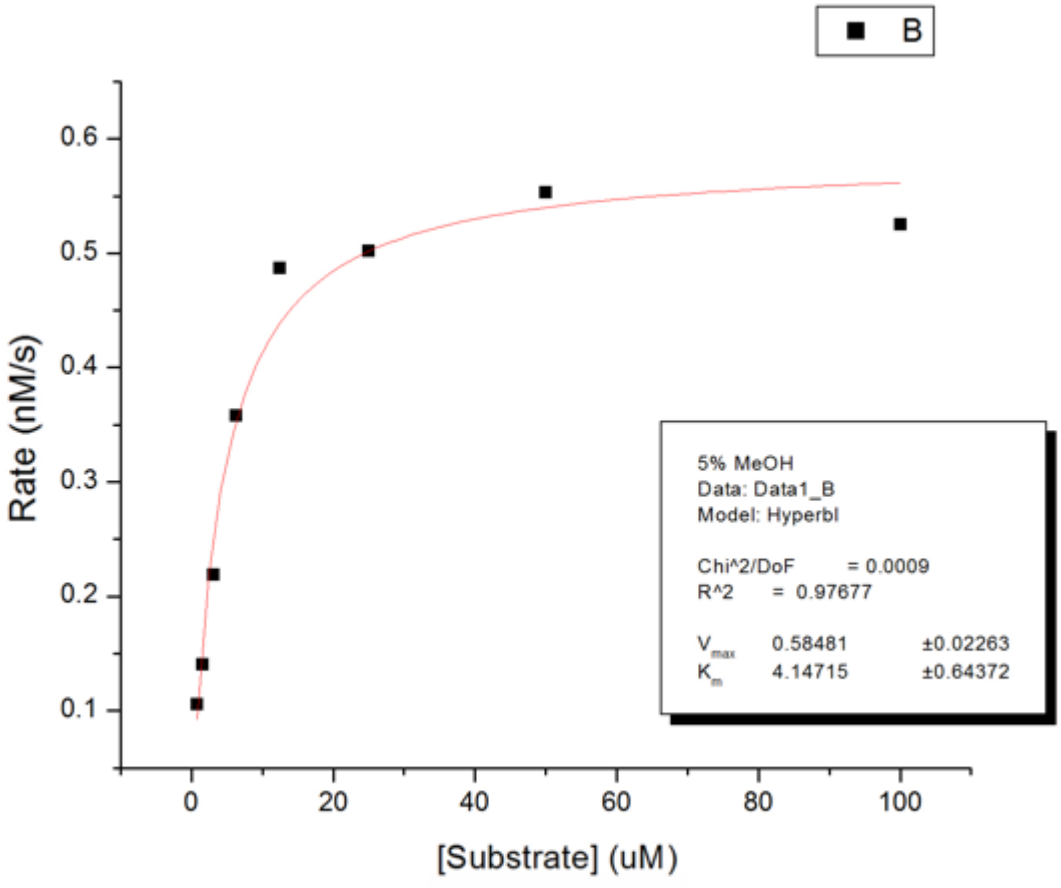
B
Rate (nM/s)
0.6
0.5
0.4
0.3
0.2
0.1
0
20
40
60
80
100
[Substrate] (uM)
5% MeOH
Data: Data1_B
Model: Hyperbl
Chi^2/DoF = 0.0009
R^2 = 0.97677
V max 0.58481 ±0.02263
K m 4.14715 ±0.64372

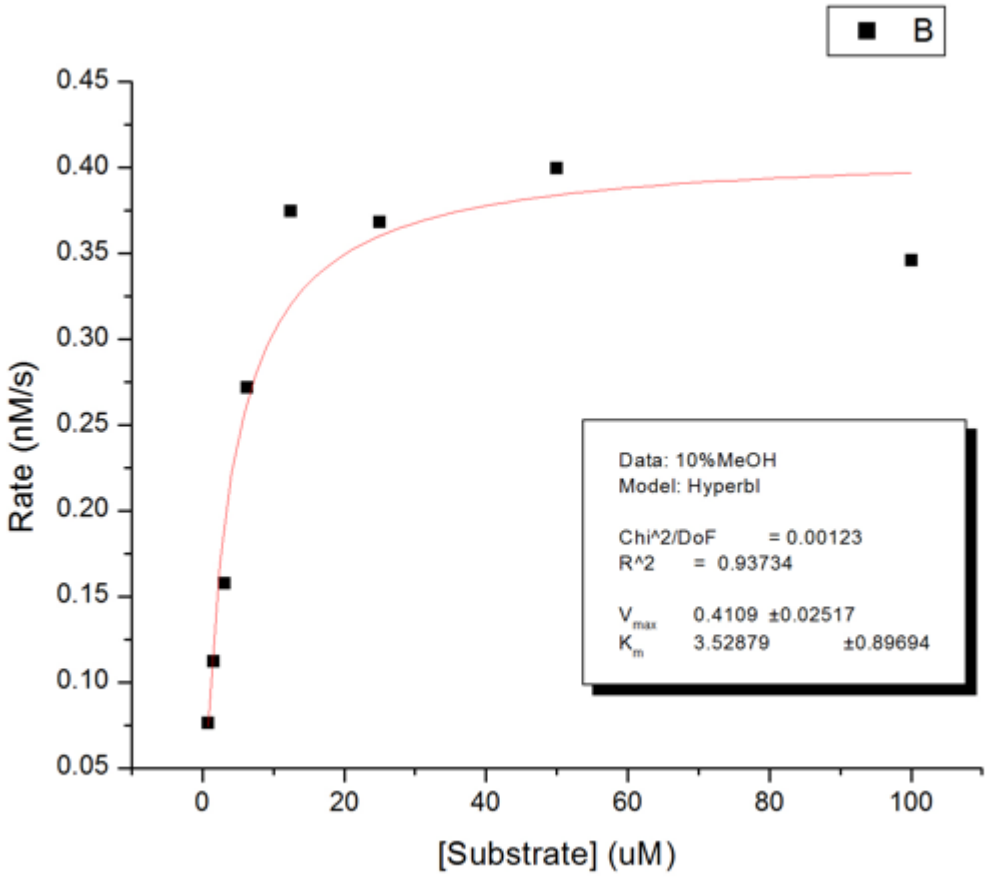
B
0.45
0.40
0.35
0.30
0.25
0.20
0.15
0.10
0.05
Rate (nM/s)
0
20
40
60
80
100
[Substrate] (uM)
Data: 10%MeOH
Model: Hyperbl
Chi^2/DoF = 0.00123
R^2 = 0.93734
V max 0.4109 ±0.02517
K m 3.52879 ±0.89694

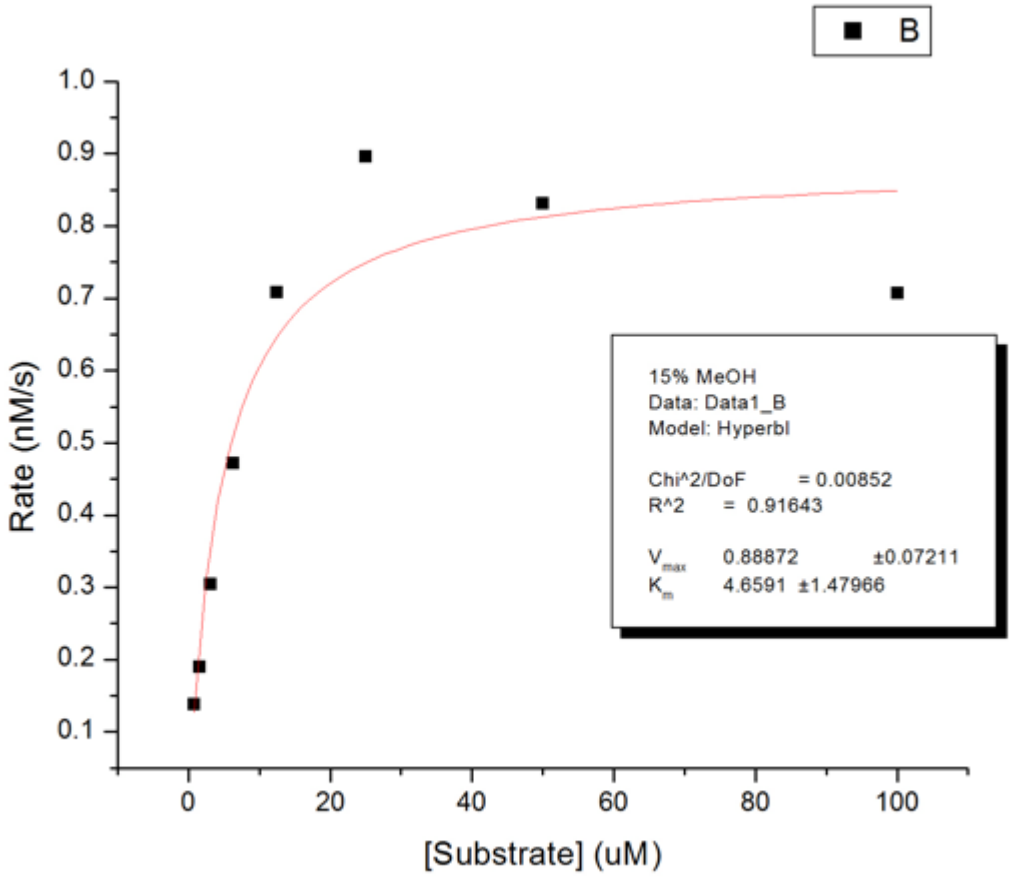
B
1.0
0.9
0.8
0.7
0.6
0.5
0.4
0.3
0.2
0.1
Rate (nM/s)
0
20
40
60
80
100
[Substrate] (uM)
15% MeOH
Data: Data1_B
Model: Hyperbl
Chi^2/DoF = 0.00852
R^2 = 0.91643
V_max 0.88872 ±0.07211
K_m 4.6591 ±1.47966

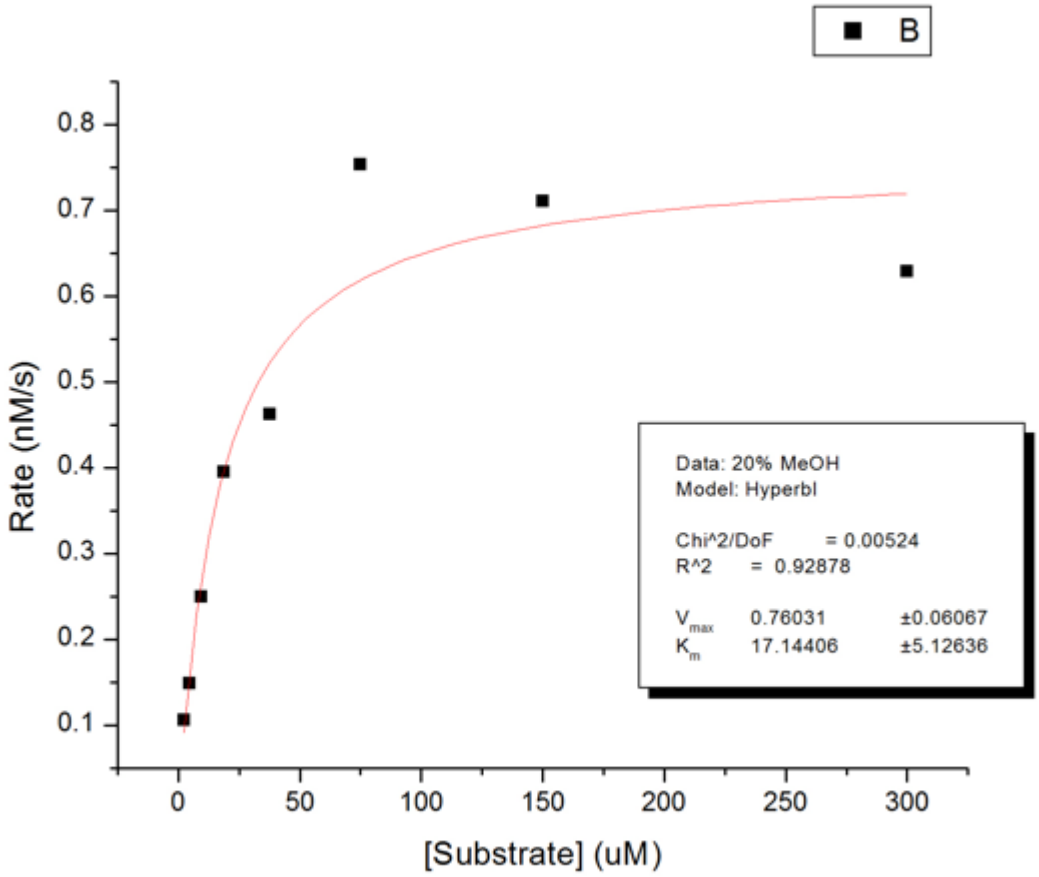
B
Rate (nM/s)
0.8
0.7
0.6
0.5
0.4
0.3
0.2
0.1
0
50
100
150
200
250
300
[Substrate] (uM)
Data: 20% MeOH
Model: Hyperbl
Chi^2/DoF = 0.00524
R^2 = 0.92878
V max 0.76031 ±0.06067
K m 17.14406 ±5.12636

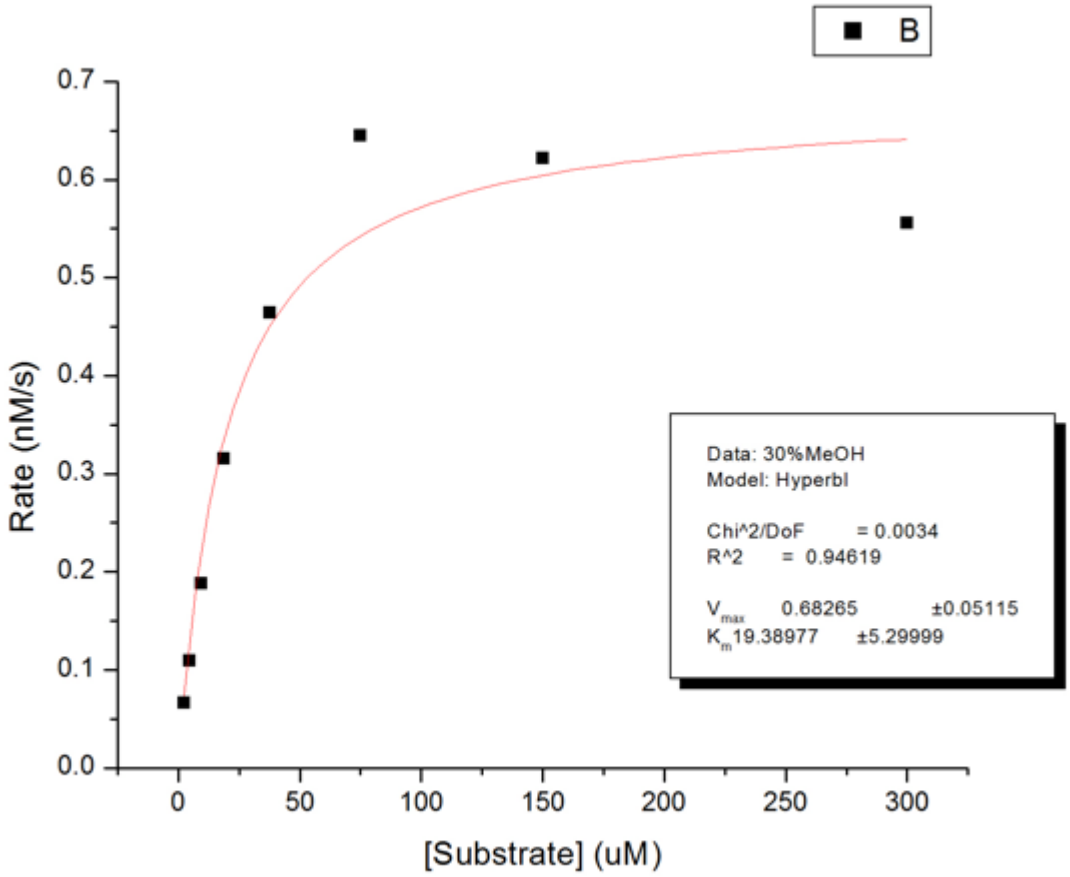

Ethanol

[EtOH]	k_{cat} (s^{-1})	k_{cat} error	K_m (μM)	K_m error	k_{cat}/K_m ($\mu M^{-1}s^{-1}$)	K_{cat}/K_m error
0%	0.00757	0.00018	3.95707	0.37102	0.00191	0.00018
10%	0.01360	0.00093	3.37995	0.96705	0.00402	0.00118
15%	0.01146	0.00091	4.13205	1.31909	0.00277	0.00091
20%	0.01244	0.00105	6.84770	2.08697	0.00182	0.00057
30%	0.01662	0.00088	19.33826	2.85259	0.00086	0.00013

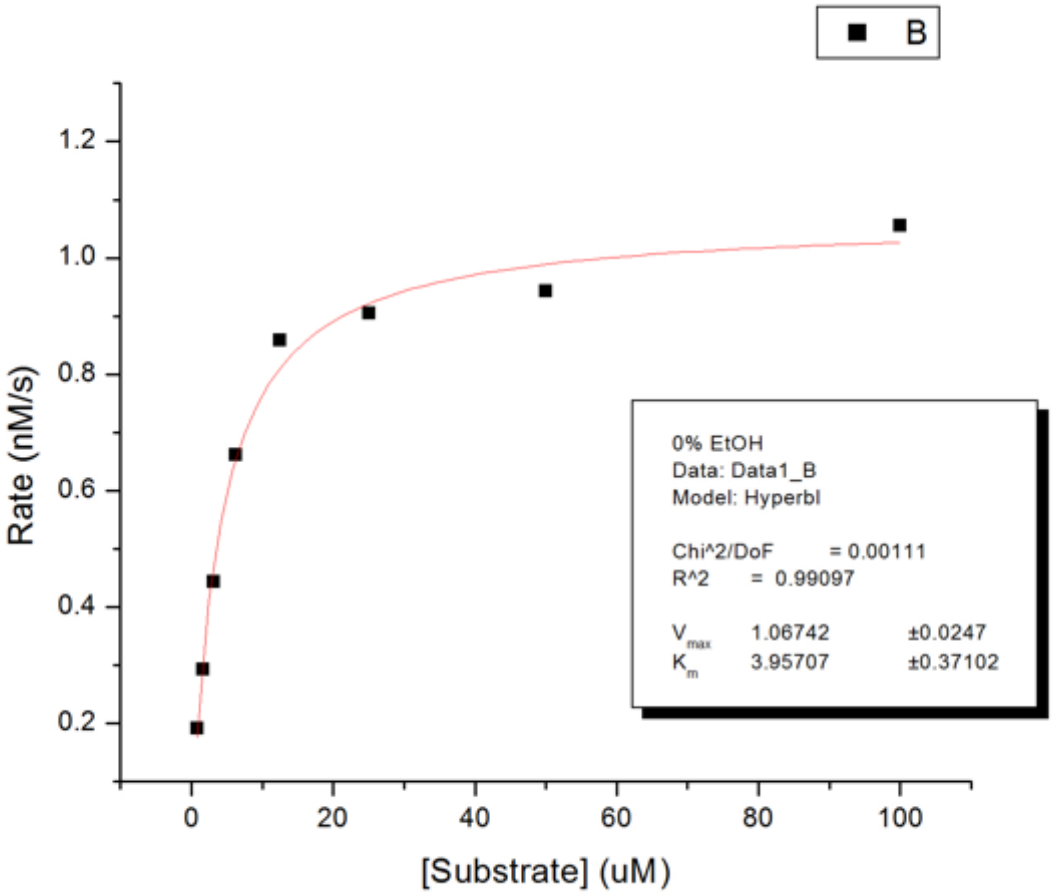
B
Rate (nM/s)
1.2
1.0
0.8
0.6
0.4
0.2
0
20
40
60
80
100
[Substrate] (uM)
0% EtOH
Data: Data1_B
Model: Hyperbl
Chi^2/DoF = 0.00111
R^2 = 0.99097
V max 1.06742 ±0.0247
K m 3.95707 ±0.37102

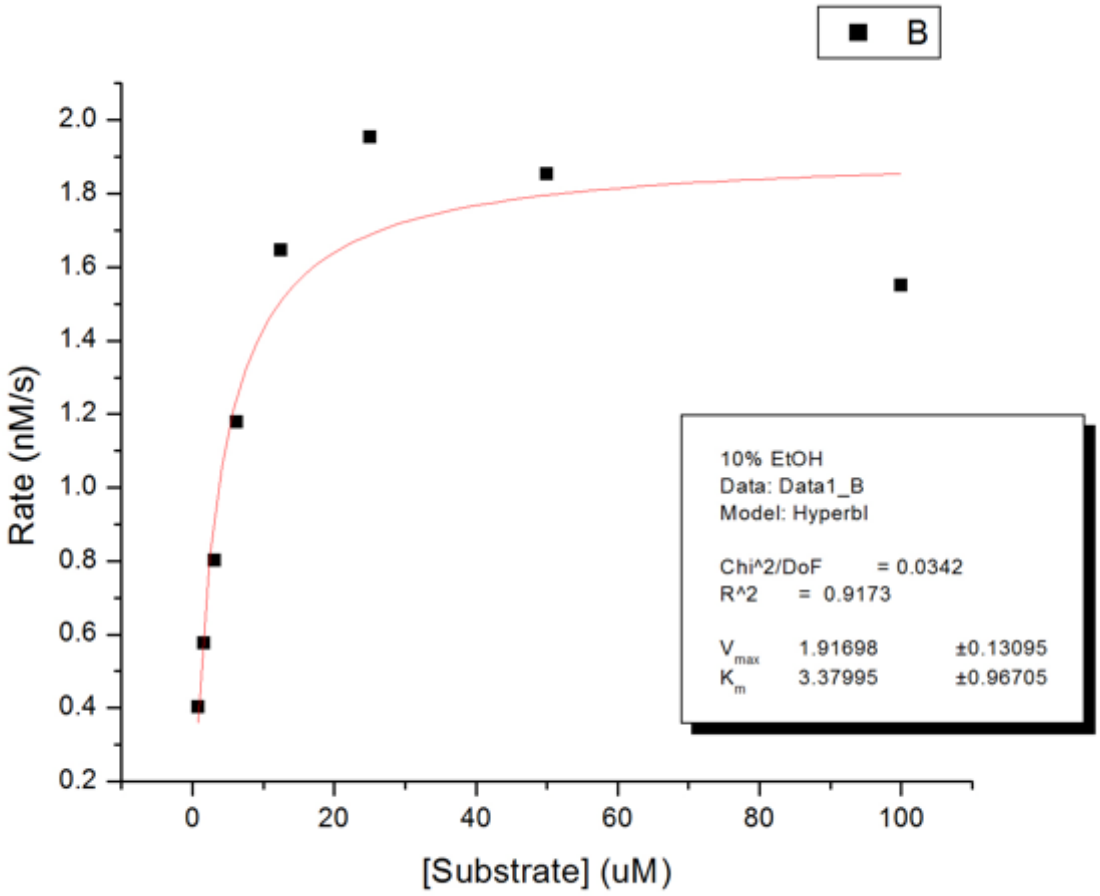
B
Rate (nM/s)
2.0
1.8
1.6
1.4
1.2
1.0
0.8
0.6
0.4
0.2
0
20
40
60
80
100
[Substrate] (uM)
10% EtOH
Data: Data1_B
Model: Hyperbl
Chi^2/DoF = 0.0342
R^2 = 0.9173
V max 1.91698 ±0.13095
K m 3.37995 ±0.96705

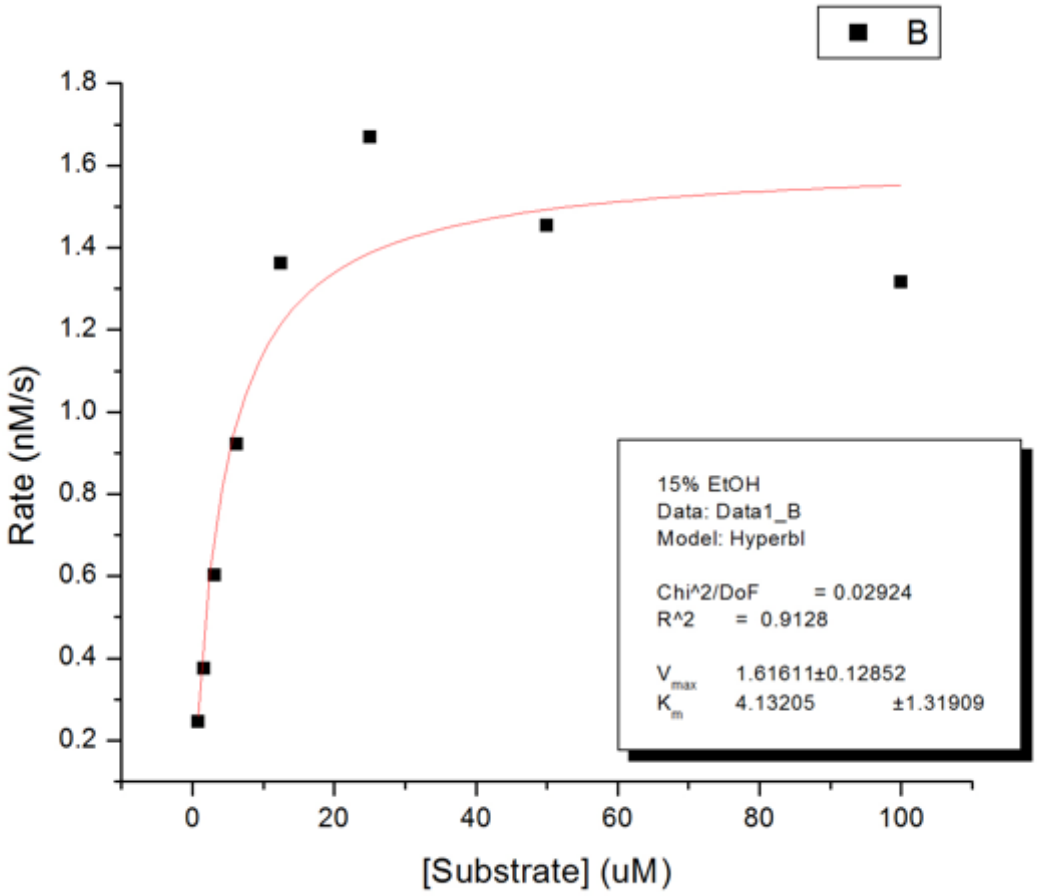
B
Rate (nM/s)
[Substrate] (uM)
15% EtOH
Data: Data1_B
Model: Hyperbl
Chi^2/DoF = 0.02924
R^2 = 0.9128
V max 1.61611±0.12852
K m 4.13205 ±1.31909

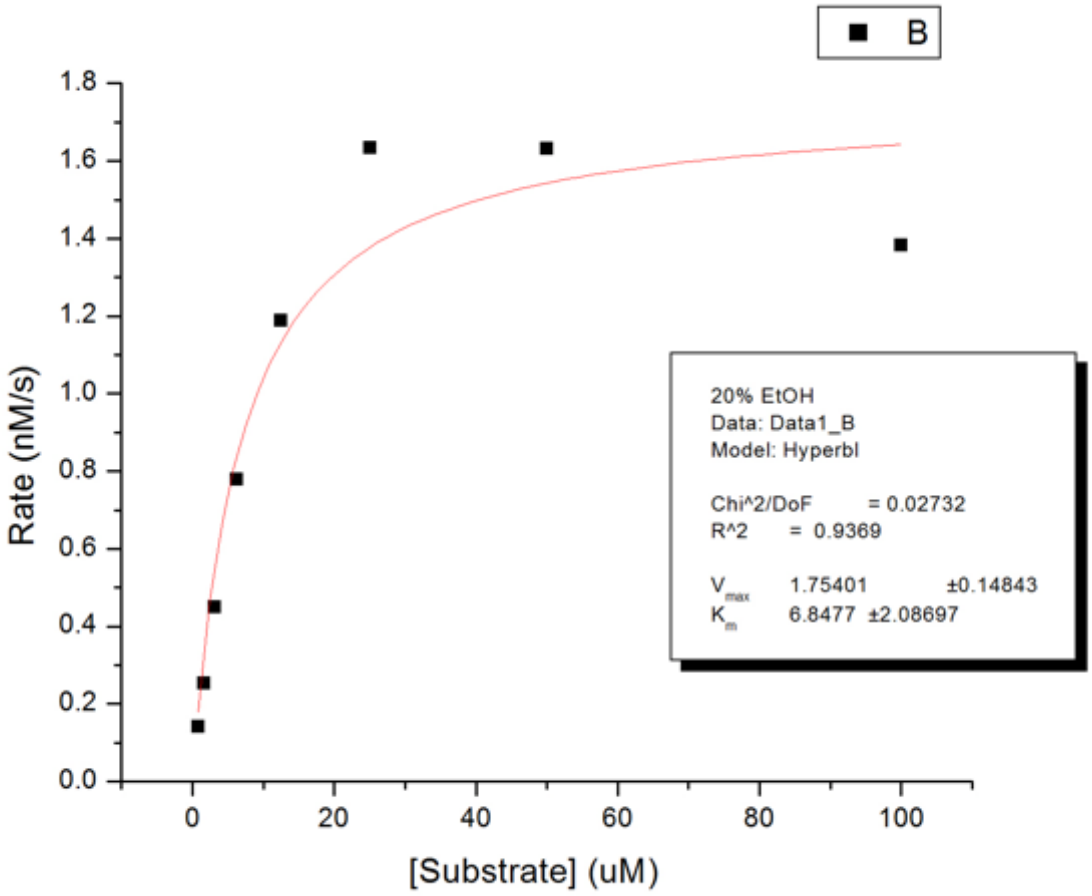
B
Rate (nM/s)
[Substrate] (uM)
0.0
0.2
0.4
0.6
0.8
1.0
1.2
1.4
1.6
1.8
0
20
40
60
80
100
20% EtOH
Data: Data1_B
Model: Hyperbl
Chi^2/DoF = 0.02732
R^2 = 0.9369
V max 1.75401 ±0.14843
K m 6.8477 ±2.08697

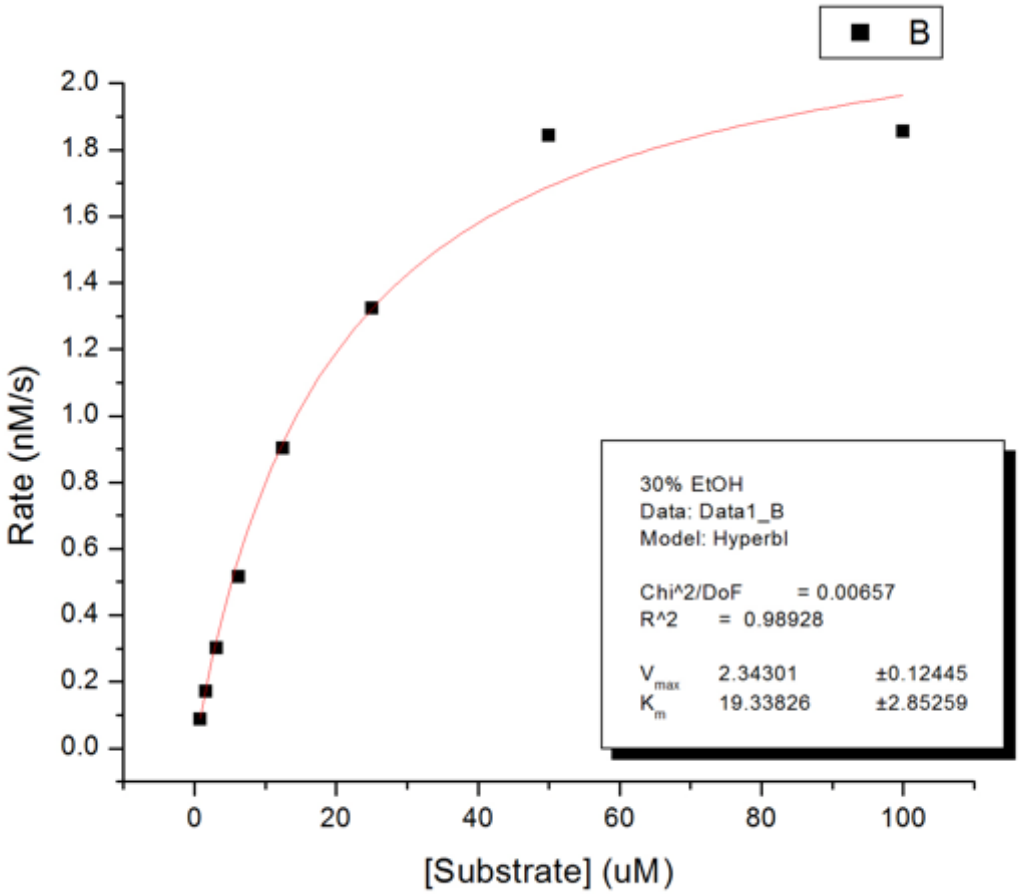

Isopropanol

[OH]	K_{cat} (s^{-1})	K_{cat} error	K_m (μM)	K_m error	k_{cat}/K_m ($\mu M^{-1}s^{-1}$)	k_{cat}/K_m error
0%	0.00241	0.00011	7.09344	1.17929	0.00034	0.00006
10%	0.00549	0.00055	5.30474	2.01568	0.00103	0.00041
20%	0.00688	0.00086	11.28140	4.50526	0.00061	0.00026
25%	0.00510	0.00045	20.74800	4.93760	0.00025	0.00006
30%	0.00262	0.00025	8.78703	2.83314	0.00030	0.00010

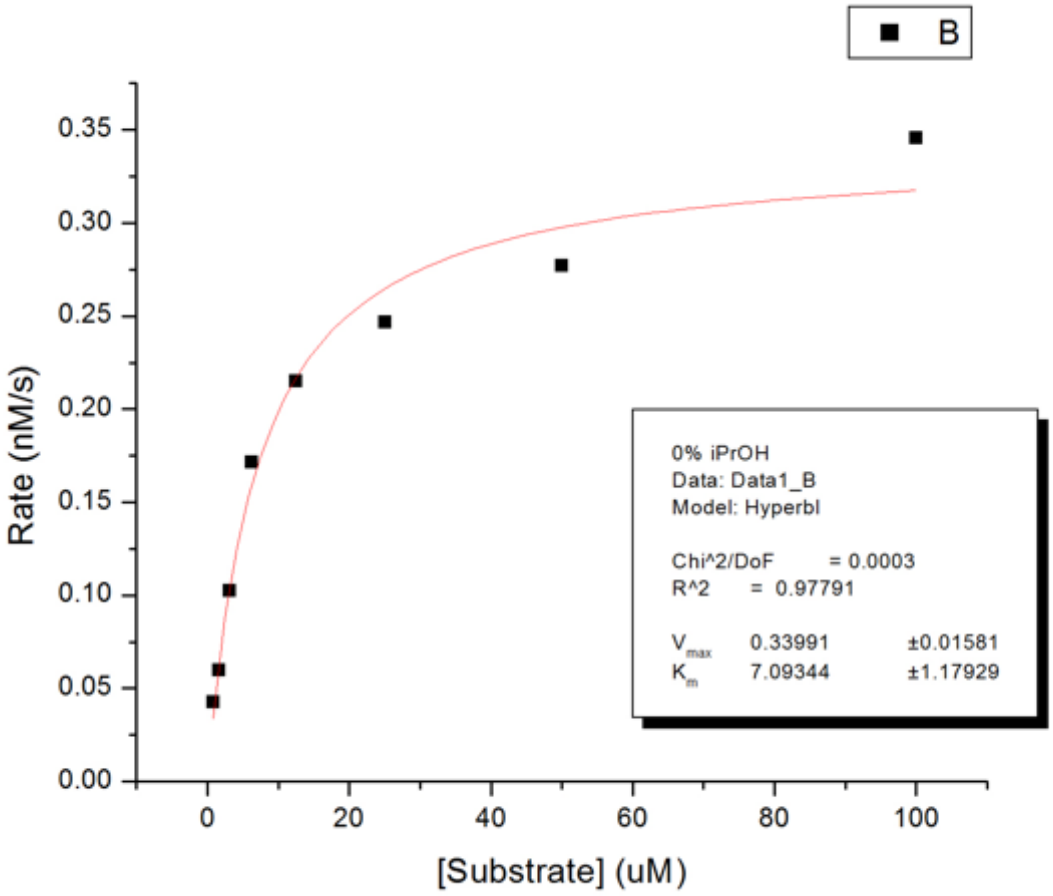
B
Rate (nM/s)
0.35
0.30
0.25
0.20
0.15
0.10
0.05
0.00
0
20
40
60
80
100
[Substrate] (uM)
0% iPrOH
Data: Data1_B
Model: Hyperbl
Chi^2/DoF = 0.0003
R^2 = 0.97791
V max 0.33991 ±0.01581
K m 7.09344 ±1.17929

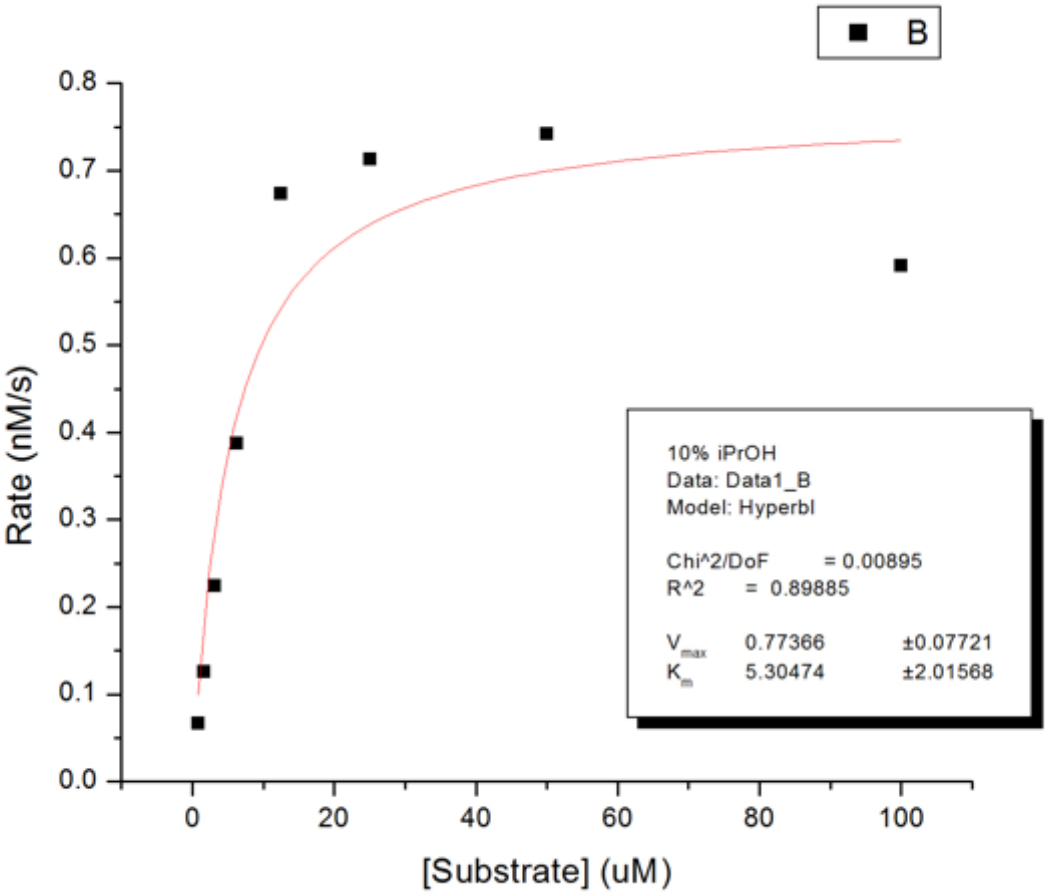
B
Rate (nM/s)
0.0
0.1
0.2
0.3
0.4
0.5
0.6
0.7
0.8
0
20
40
60
80
100
[Substrate] (uM)
10% iPrOH
Data: Data1_B
Model: Hyperbl
Chi^2/DoF = 0.00895
R^2 = 0.89885
Vmax 0.77366 ±0.07721
Km 5.30474 ±2.01568

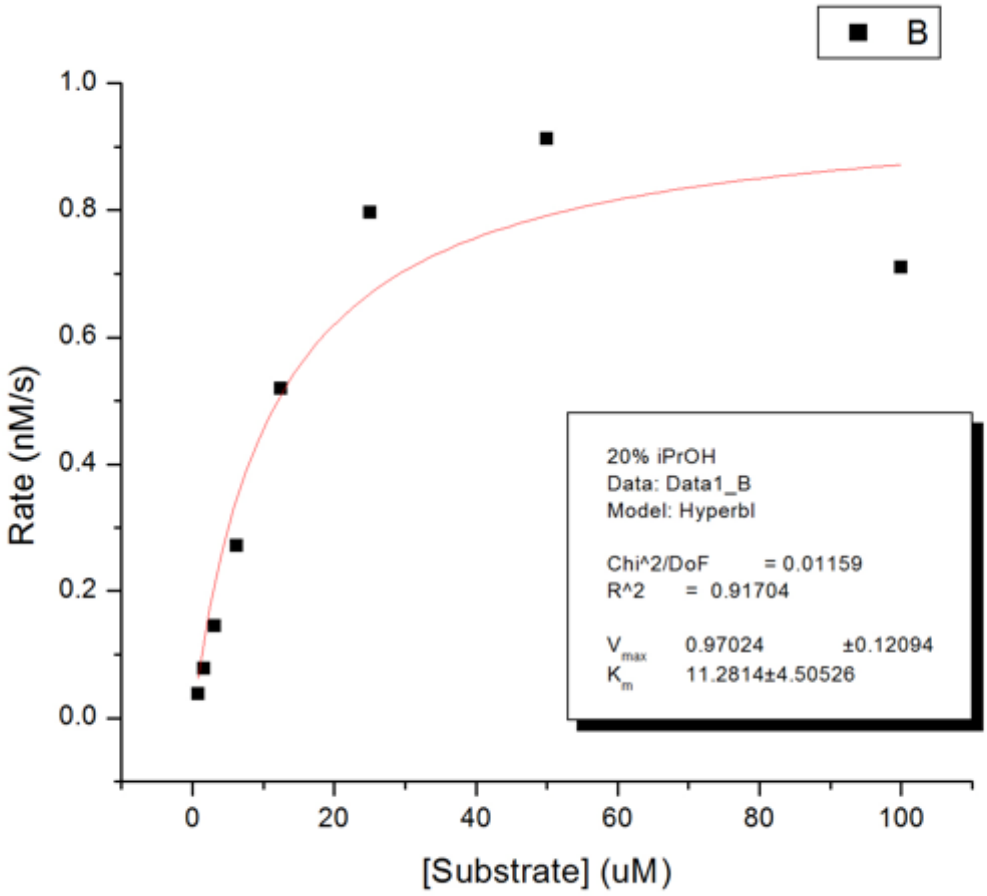
B
1.0
0.8
0.6
0.4
0.2
0.0
Rate (nM/s)
0
20
40
60
80
100
[Substrate] (uM)
20% iPrOH
Data: Data1_B
Model: Hyperbl
Chi^2/DoF = 0.01159
R^2 = 0.91704
V max 0.97024 ±0.12094
K m 11.2814±4.50526

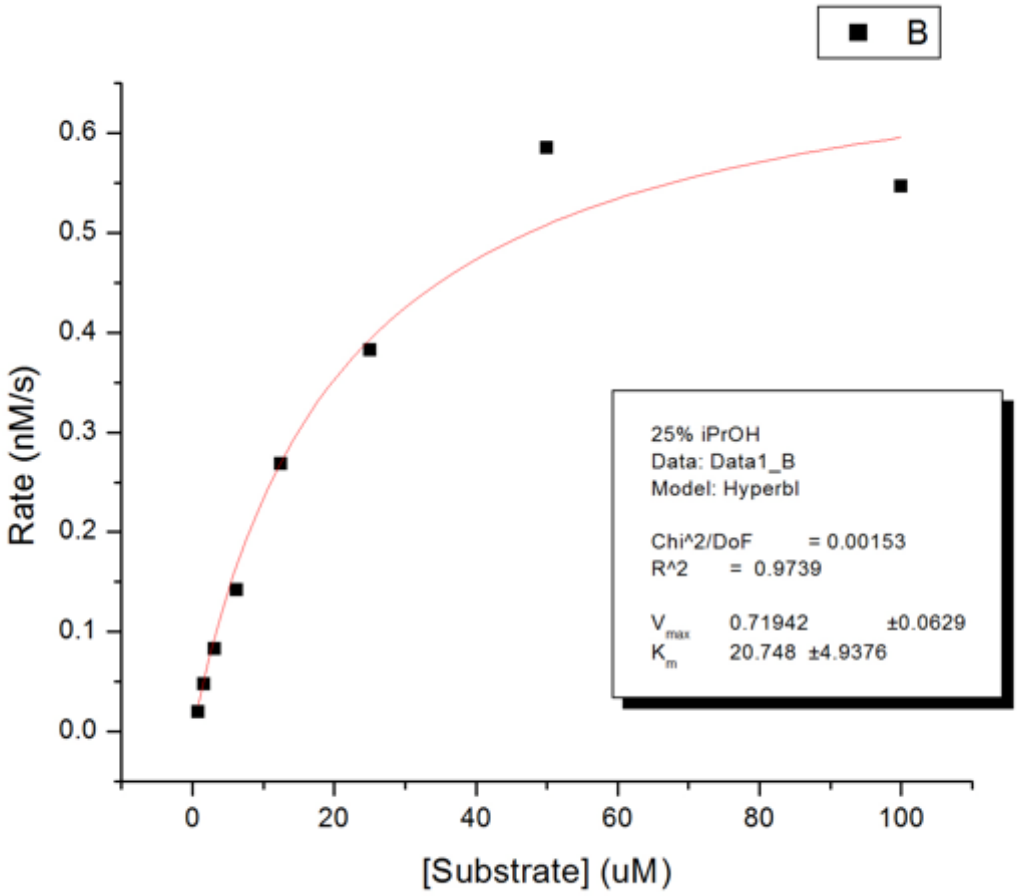
B
Rate (nM/s)
0.0
0.1
0.2
0.3
0.4
0.5
0.6
0
20
40
60
80
100
[Substrate] (uM)
25% iPrOH
Data: Data1_B
Model: Hyperbl
Chi^2/DoF = 0.00153
R^2 = 0.9739
Vmax 0.71942 ±0.0629
Km 20.748 ±4.9376

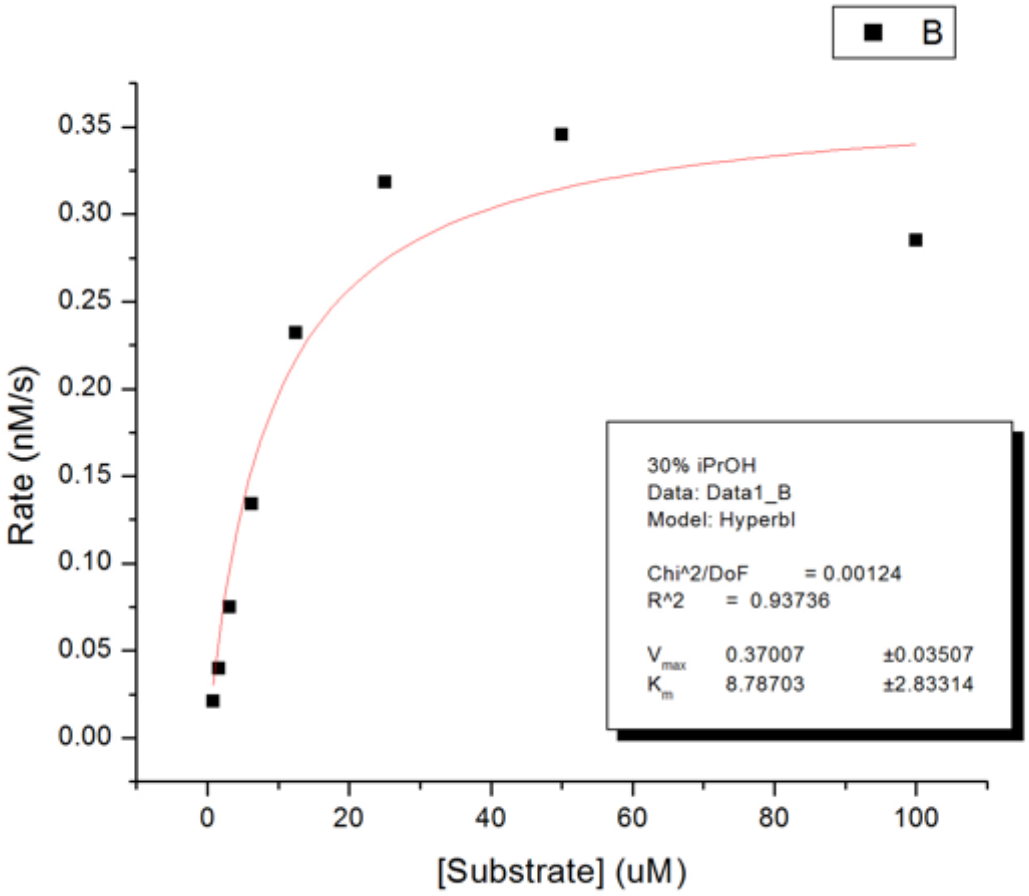
B
Rate (nM/s)
0.35
0.30
0.25
0.20
0.15
0.10
0.05
0.00
0
20
40
60
80
100
[Substrate] (uM)
30% iPrOH
Data: Data1_B
Model: Hyperbl
Chi^2/DoF = 0.00124
R^2 = 0.93736
V max 0.37007 ±0.03507
K m 8.78703 ±2.83314